

https://dspace.org/

Polymorphism in pharmaceutical co-crystals

Mnguni, Malitsatsi Jesse

2017

http://hdl.handle.net/10539/22734

Mnguni, Malitsatsi Jesse (2017) Polymorphism in pharmaceutical co-crystals, University of the Witwatersrand, Johannesburg, <http://hdl.handle.net/10539/22734>

Downloaded from a DSpace repository. https://dspace.org/



UNIVERSITY OF THE
WITWATERSRAND,
JOHANNESBURG

Polymorphism in Pharmaceutical Co-crystals

Malitsatsi Jesse Mnguni

Supervisors: Prof. A. Lemmerer

Prof. J. Michael

A Dissertation submitted to the Faculty of Science, University of the Witwatersrand, Johannesburg, in fulfilment of the requirements for the degree of Master of Science

6 February 2017, Johannesburg

Declaration

I, Malitsatsi Jesse Mnguni, declare that this Dissertation is my own, unaided work. It is being submitted for the Degree of Master of Science at the University of the Witwatersrand, Johannesburg. It has not been submitted before for any degree or examination at any other University.

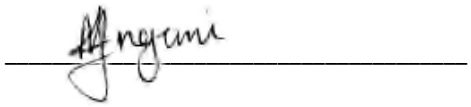

(Signature of candidate)

6th day of February _in 2017

Abstract

Polymorphism is not only limited to single component systems. Co-crystals have exhibited polymorphism and various polymorphic co-crystals have been reported. Polymorphism in co-crystals presents an expansion of the optimization space around a pharmaceutical compound and also offers the opportunity to develop novel patentable material. Polymorphism of pharmaceutical co-crystals was investigated by means of an exhaustive data mining survey and the formation of polymorphic co-crystals. The search was performed using the Cambridge Structural Database (CSD). The search aimed to find and tally neutral pharmaceutical co-crystals which are polymorphic. The survey of the CSD showed that 14% of the pharmaceutical co-crystals were polymorphic. The co-crystal of theophylline and 3,4-dihydroxybenzoic acid was found to be polymorphic and the novel polymorph was synthesized and characterized. The co-crystals were characterized by x-ray crystallographic techniques and Differential Scanning Calorimetry. The single crystals of carbamazepine and cinnamic acid was grown and characterized by SCXRD for the first time. The single crystal data was able to show that the hydrogen bonding packing that was modelled in the literature is incorrect.

Acknowledgements

Special acknowledgements are given to Prof. Andreas Lemmerer and Prof. Joseph P. Michael for all the guidance and support. Additional thanks are also given to the National Research Foundation (SFH14061870163) for supporting this work, and the University of the Witwatersrand as well as the School of Chemistry.

List of Abbreviations

API	Active Pharmaceutical Ingredient
CIN	Cinnamic acid
CSD	Cambridge Structural Database
DHB	Dihydroxybenzoic acid
DSC	Differential Scanning Calorimetry
GRAS	Generally Regarded as Safe
HMS	Hot Stage Microscopy
PXRD	Powder X-Ray Diffraction
SXRD	Single Crystal X-Ray Diffraction
TPL	Theophylline

List of Tables

Table 1: Melting points of co-crystals and co-formers used in study by Aakeröy and co-workers.[19] 6
Table 2: Amount of curcumin dissolved in 40% ethanol/water at 37°C over a period of 4 hours when starting from different solid-state forms.[24] 7
Table 3: List of the active pharmaceutical ingredients used in the project along with the co-formers used for the polymorphism screen. 33
Table 4: Observed interactions between theophylline and various dihydroxybenzoic acid co-formers. 40
Table 5: Crystallographic Data for Forms I and II of (TPL)·(3,4-DHB) 42
Table 6: Temperatures of the melting and transition endotherms. 45
Table 7: Crystallographic data for (carbamazepine)·(cinnamic acid) 52

List of Figures

Figure 1: Flow diagram showing the different types of crystalline solids. Adapted from Steed[5] and Aitipamula *et. al*. [6] 2
Figure 2: Diagram showing the different classes in the biopharmaceutics classification system.[11] 4
Figure 3: The hydrogen bond. The red dashed line indicates the intermolecular interaction and the black solid line a covalent bond. The interaction angle ($\angle \mathbf{D} - \mathbf{H} \cdots \mathbf{A}$) is labelled as θ and the hydrogen··· acceptor (H···A) distance as *d.* 9
Figure 4: Different types of hydrogen bonding interactions. (a). The standard interaction with one acceptor. (b) Bifurcated interaction with two acceptors. (c) The trifurcated interaction with three acceptors. 10
Figure 5: Infographic depicting supramolecular synthesis and covalent synthesis analogy. 11
Figure 6: Plot showing the number of compounds that had one or more polymorphin a screen carried out on 245 compound by SSCI(Reproduced from Stahly).[15] 14
Figure 7: Energy-temperature diagrams for the enantiotropic (left) and monotropic (right) systems for solid phases of polymorphs A and B.[41] 15
Figure 8: Diagrammatic representation of polymorphs in single and multi-component crystals. 16
Figure 9: Synthon polymorphism in 2,3,5,6-tetramethylpyrazine and 4-hydroxybenzoic acid co-crystals.[50] (a) Hydrogen bonding patterns observed in Form I of the co-crystal. (b) Hydrogen bonding patterns observed in Form II of the co-crystal. 17
Figure 10: Packing polymorphism observed in polymorphic co-crystal of 2-aminopyrimidine·benzoic acid. (a). Form I of 2-aminopyrimidine·benzoic acid co-crystal. (b) Form II of 2-aminopyrimidine·benzoic acid co-crystal. 19
Figure 11: Screenshot of *ConQuest* showing the queries and Boolean logic used to generate the hit list for database survey. 24
Figure 12: Plot showing the propensity of pharmaceutical co-crystal and polymorphs in co-crystals in a CSD study of 2925 neutral organic co-crystals. 25
Figure 13: Plot showing percentage of co-crystals that exhibited various types of polymorphism in a CSD screen of 239 polymorphic co-crystals. 26
Figure 14: The packing in the polymorphic co-crystals of *N,N'*-diacetylpiperzine and 2-hydroxybenzoic acid.[52](a)Packing diagram of form I of the co-crystal. (b) Packing diagram of form II of the co-crystal 27
Figure 15: Some examples of conformational polymorphism.[58, 59] The molecules in purple are from form I of the different co-crystals and the molecules in blue are from form II of the different co-crystals. Changes in conformation are observed

in the molecules on the left and these changes then result in the different polymorphs of the co-crystal. 28
Figure 16: Synthon polymorphism in co-crystal of 4-hydroxybenzoic acid and 4,4'-bipyridine.[60](a) Hydrogen bonding synthons observed in form I of 4-hydroxybenzoic acid·4,4'-bipyridine. (b) Hydrogen bonding synthons observed in form II of 4-hydroxybenzoic acid·4,4'-bipyridine..... 29
Figure 17: Plot showing the percentage of co-crystals that fell into different types of pharmaceutical co-crystal groups in a screen carried out on 400 pharmaceutical co-crystals found in the CSD. 30
Figure 18: The different co-formers found in the 5 polymorphic caffeine co-crystals and the type of polymorphism observed in each co-crystal..... 31
Figure 19: Single crystals of 3,4-dihydroxybenzoic acid (form I) growing on a polyethylene bead. 35
Figure 20: Asymmetric units of Forms I and II of the (TPL)·(3,4-DHB) co-crystal. The atomic numbering in the crystal structures is shown along with the non-symmetry related hydrogen bonding (indicated by the red dashed lines). 43
Figure 21: Hydrogen bonding patterns in the polymorphs of the co-crystal (Theophylline)·(3,4-dihydroxybenzoic acid). The red dashed lines represent hydrogen bonds and hydrogen atoms were excluded for clarity.(a) Hydrogen bonding in form I of the co-crystal. (b)Packing in I. (c). Hydrogen bonding in form II of the co-crystal. (d) Packing in II. 44
Figure 22: DSC traces of the polymorphs of (TPL)·(3,4-DHB). The red trace shows the heating of Form I and the purple trace shows the response of Form II to heating and a phase transition (from II to I) at 63.2°C is observed. 45
Figure 23:Thermal analysis of the different polymorphs of theophylline·3,4-dihydroxybenzoic acid performed on a hotstage. (a) Block morphology of form I of the co-crystal. (b) Needle morphology of form II of the co-crystal. (c) Heating of Form II lead to needles darkening as phase transition occurs. (d). Form I blocks formed from the form II needles upon further heating..... 46
Figure 24: (a) Carbamazepine dimer observed in carbamazepine·4-hydroxybenzoicacid form I co-crystals. (b) Heterosynthon observed in carbamazepine·4-hydroxybenzoicacid form II co-crystals. [85] 49
Figure 25: Intermolecular interactions of the carbamazepine·cinnamic acid co-crystal that were predicted by Moridiya et al. (2014). Picture taken from ref [86]. 50
Figure 26: PXRD patterns of the carbamazepine·cinnamic acid co-crystal synthesized in this work: (a) Measured powder pattern of the co-crystal (measured using cobalt radiation). (b) Calculated powder pattern of carbamazepine·cinnamic acid co-crystal using cobalt radiation. 53
Figure 27: Powder patterns of the carbamazepine·cinnamic acid co-crystal taken from different sources: (a) Carbamazepine·cinnamic acid co-crystal powder pattern taken from ref 25. (b) Carbamazepine·cinnamic acid co-crystal powder

pattern taken from ref 88. (c) Calculated powder pattern of carbamazepine·cinnamic acid co-crystal using copper radiation. 54
Figure 28: DSC thermogram of co-crystal of cinnamic acid and carbamazepine. 55
Figure 29: The asymmetric unit of the co-crystal with the displacement ellipsoid drawn at 50% probability level. 55
Figure 30: Hydrogen bonding interactions in carbamazepine·cinnamic acid. 56
Figure S1: PXRD of TPL·3,4-DHB form I compared to PXRD of single crystal structure determination of TPL·3,4-DHB form. The experimental pattern was calculated at room temperature and the calculated pattern at 173 K. 64
Figure S2: PXRD of TPL·3,4-DHB form II compared to PXRD of single crystal structure determination of TPL·3,4-DHB form. The experimental pattern was calculated at room temperature and the calculated pattern at 173 K 64

Table of Contents

Declaration i
Abstract ii
Acknowledgements iii
List of Abbreviations iv
List of Tables v
List of Figures vi
1. Introduction: Solids and the Pharmaceutical Industry 1
1.1. The Crystalline Solid State 1
1.2. Co-Crystals 3
1.2.1. What is a Co-crystal? 4
1.2.2. Prevalence of Co-crystals 5
1.3. Physicochemical Properties of Co-crystals 5
1.3.1. Melting Point 5
1.3.2. Stability 6
1.3.3. Solubility 7
1.4. Designing Co-crystals: Crystal Engineering 8
1.4.1. Intermolecular Interactions 8
1.4.2. The Hydrogen Bond 9
1.4.3. Supramolecular Synthons and Retrosynthesis 10
1.5. Polymorphism 13
1.5.1. Thermodynamics 14
1.5.2. Polymorphism in the Pharmaceutical Industry 15
1.5.3. Polymorphism in Co-crystals 15
1.5.4. Classification of Co-crystal Polymorphs 16
1.6. The Cambridge Structural Database 19
1.7. Aims 20
2. The Hunt for Polymorphic Co-Crystals 21
2.1. Introduction 21
2.2. Methodology 21
2.3. Results 25
2.3.1. Polymorphic Co-crystals 25

2.3.2. Pharmaceutical Co-crystals 29
3. Methods and Materials 32
3.1. Polymorph Screening Techniques 33
3.1.1. Slow Evaporation 34
3.1.2. Slow cooling 34
3.1.3. Solvent-Assisted Grinding 34
3.1.4. Heterogeneous Seeding 34
3.2. Instrumentation 35
3.2.1. Single Crystal X-Ray Diffraction (SXRD) 35
3.2.2. Powder X-Ray Diffraction (PXRD) 36
3.2.3. Differential Scanning Calorimetry (DSC) 36
3.2.4. Hot Stage Microscopy (HSM) 36
4. Co-Crystals of Theophylline 37
4.1. Synthon Competition in Co-crystals of Theophylline 37
4.2. Polymorphic Co-Crystal of Theophylline and 3,4-Dihydroxybenzoic acid. 40
4.2.1. Experimental 41
4.2.2. Crystal Structures of the polymorphs of (TPL)·(3,4-DHB) 43
4.2.3. Thermal Studies of (TPL)·(3,4-DHB) Polymorphs. 44
5. Co-crystal of Carbamazepine 48
5.1. Introduction 48
5.2. Co-crystal: Carbamazepine●Cinnamic acid 50
5.2.1. Experimental 50
5.2.2. Powder Analysis 53
5.2.3. Thermal Analysis 54
5.2.4. Structural Analysis 55
6. Concluding Remarks 57
6.1. Remarks on the data mining 57
6.2. Targeted attempts to form synthon polymorphs 58
6.2.1. Theophylline co-crystals 58
6.2.2. Carbamazepine co-crystals 59
References 60
Supporting Information 63
1.1. Supporting information for TPL 3,4DHB polymorphs 64

1.2.1. Powder diffraction patterns of Form I and II of TPL·3,4-DHB.....64

1. Introduction: Solids and the Pharmaceutical Industry

There are many drugs on the shelves of pharmacies and more are still being developed for multiple reasons. Of all the lead compounds that are currently under development, only 1% of those potential drugs will make it onto the shelves.[1, 2] These poor laboratory-to-market turnover rates are due to many setbacks and pitfalls during the drug development journey. Some of the chief issues attributed to the discarding of a lead compound are related to the compound's properties in the solid state.[3] Bioavailability (highly influenced by the dissolution rate), solubility, stability and other physical properties are some of the troublesome properties that need to be optimised early in drug development in order to increase the lead compound's chance of success.[1]

1.1. The Crystalline Solid State

The solid state comes in many forms. Understanding the difference between these forms is fundamental to knowing which solid form to opt for during drug development. Knowledge about the chosen solid form can drastically reduce the amount of time taken during the early drug development stage and ultimately reduce the costs of drug development.[4] Usually, crystalline solids are targeted first because crystalline solids are more thermodynamically stable than their amorphous counterparts.[4] There are many different types of crystalline materials including (but not limited to) salts, co-crystals and clathrates. Figure 1 gives a basic overview of what these crystalline solids are and how they are related.

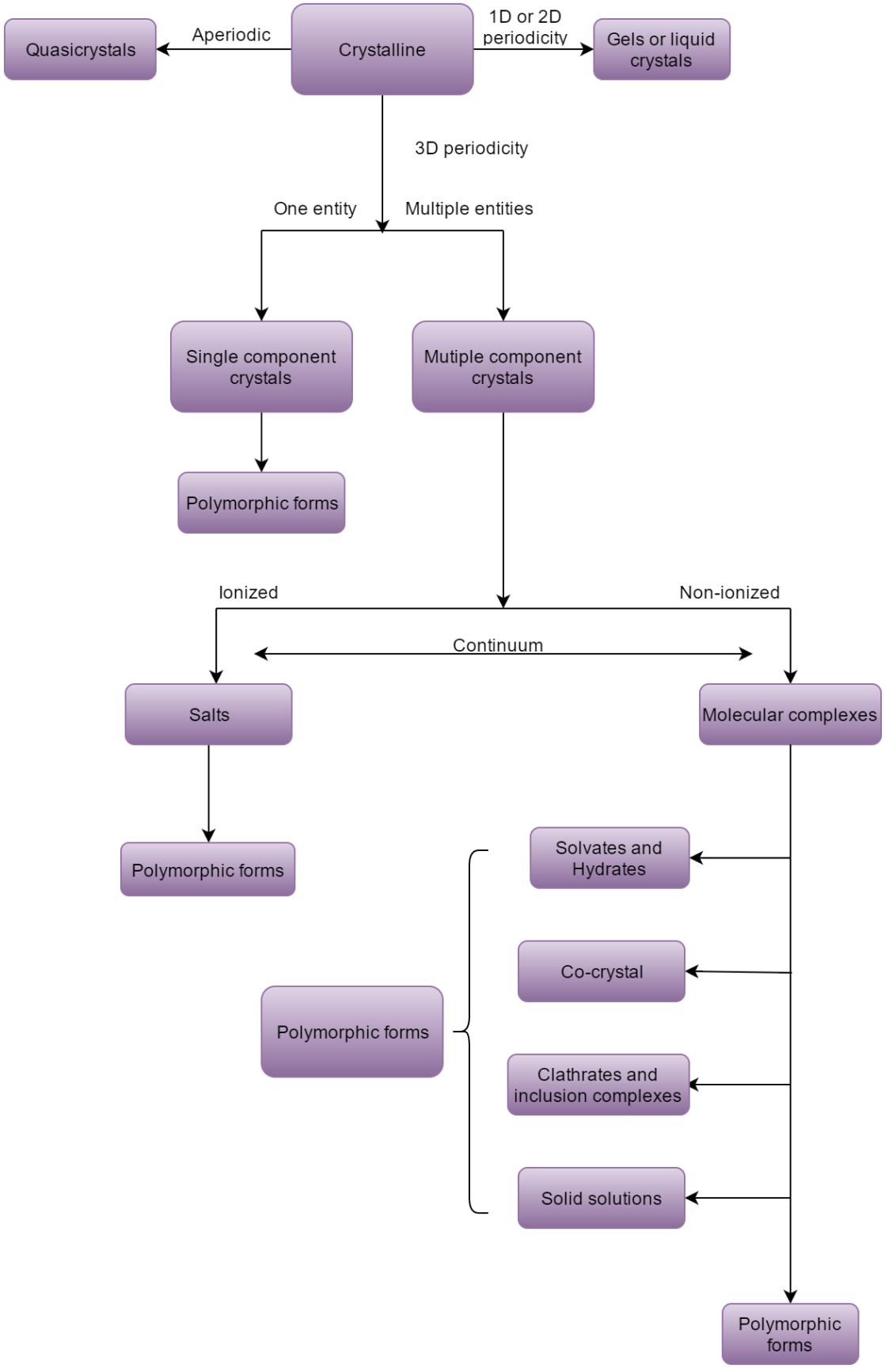

Figure 1: Flow diagram showing the different types of crystalline solids. Adapted from Steed[5] and Aitipamula *et. al.* [6]

Crystalline materials derive some of their physical properties from their molecular arrangement within the crystal.[1] Altering the arrangement of these molecules and the interactions alters the physical properties of these solids.[1] This principle is used extensively in attempts to improve properties of pharmaceuticals. Opting for alternative solid forms is a well-established technique in the pharmaceutical industry.[7] These improvements can be anything from altering the melting point to changing the taste of the medicine.[2] For example, bitter drugs can be made more palatable by using inclusion complexes such as β-cyclodextrin .[4] These complexing agents are able to make drugs appear less bitter tasting by either decreasing the solubility of the drug upon ingestion or by weakening the drug – taste bud interaction.

1.2. Co-Crystals

Crystallization is known for being a method of molecular exclusion and recrystallizations are frequently used to purify compounds. Performing crystallization experiments in order to include other molecules is counter-intuitive and is referred to as co-crystallization which leads to what is called a multi-component molecular complex or co-crystal.[8, 9]

In the past pharmaceutical companies have used salts to improve the active pharmaceutical ingredients (API) properties and as a result 50% of the medicines on the market are still delivered as salts.[4] Salts are chemical compounds comprising an assembly of cations and anions.[10] Co-crystals, just like salts, can provide an improvement of the unfavourable properties of pharmaceuticals. Co-crystals also offer the additional advantages of the nullification of the ionizable centre requirement that is present for salt formation.[2] This opens up the possibility for non-ionizable drugs that were discarded because of poor properties, to be reformulated.

The increase in co-crystal research has been propelled by the fact that approximately 70-80% of the drugs currently under development are classified as Class 2 or Class 4 by the biopharmaceutics classification system.[1, 4] Class 2 drugs are compounds that show low solubility and high permeability (Figure 2).[1, 4] Class 4 drugs are compounds with low solubility and low permeability.[4] These compounds, particularly class 2, are

of interest with respect to co-crystals because a co-crystal could possible increase the solubility of these compounds.

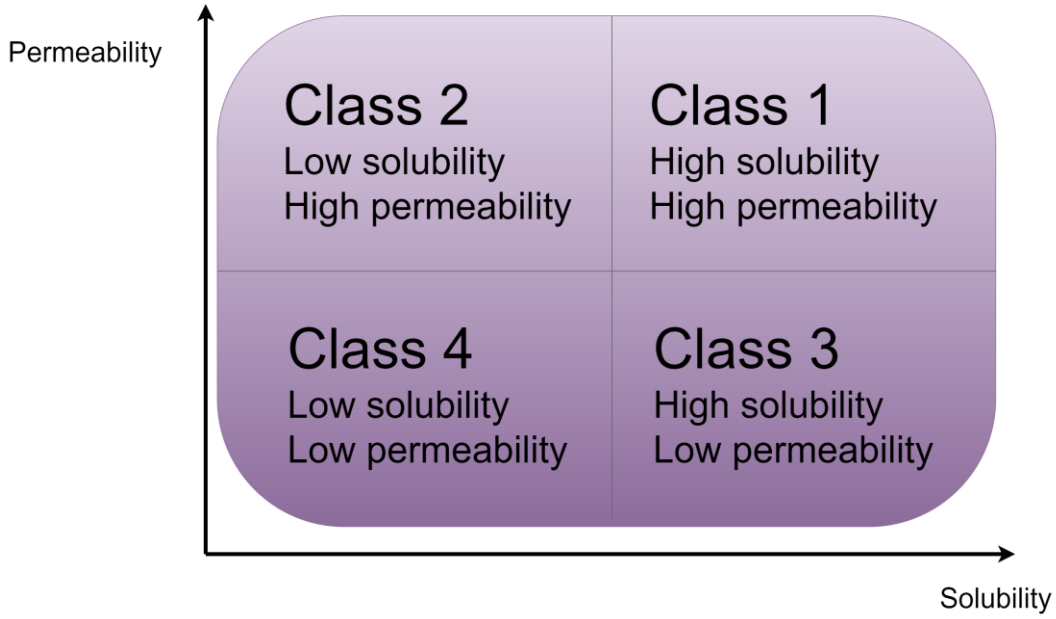

Figure 2: Diagram showing the different classes in the biopharmaceutics classification system.[11]

1.2.1. What is a Co-crystal?

Currently, there is no universally accepted definition of a co-crystal.[6] A broad definition is that a co-crystal is a crystalline material with two or more different molecules within its crystal lattice.[5, 9] This broad definition includes all multi-component crystals such as solvates, hydrates, inclusion complexes and others; whether or not all these solids are indeed co-crystals in still up for debate.[12, 13] To narrow the scope of co-crystal research, many researchers have included some restrictions on their definition of a co-crystals.[5] These restrictions commonly include:

i. Stoichiometric ratio of entities in the crystal;
ii. Entities must be solid at ambient conditions.

The first restriction excludes non-stoichiometric inclusion complexes such as urea channel clathrates. The second restriction excludes solvates and hydrates from the co-crystal definition. The trouble with restriction (ii) becomes the inherent difference in ambient conditions in different laboratories. These laboratories will then define

different compounds as co-crystals. Even though there is general intuitive consensus that some compounds (such as crystals of racemic compounds, which contain equal amounts of opposite enantiomers)[5] are not co-crystals, the question of 'what is a co-crystal?' remains unanswered. For this work, the definition that will be employed is the definition put forward by Jones[14] which defines a co-crystal as "*a crystalline complex of two or more neutral molecular constituents bound together in a crystal lattice through non-covalent interactions, often including hydrogen bonding*." In pharmaceutical co-crystals the constituents are a drug compound and another molecule often called a co-former. The co-formers used in pharmaceutical co-crystals are normally substances which are categorised as "generally regarded as safe (GRAS)" as they can be used as food additives.[2]

1.2.2. Prevalence of Co-crystals

A study done by the company SSCI attempted to gauge the prevalence of co-crystals and other solid forms.[5, 15] Although, the study had a small sample size, the results they obtained are a good indication of the prevalence of co-crystals, polymorphs and other solid-state forms. SSCI found that from 245 polymorph screens, 91% of the compounds had more than one crystal form and approximately 50% had two or more polymorphs. From 64 co-crystal screens, 61% of the compounds formed co-crystals and about one third formed solvates or hydrates.

1.3. Physicochemical Properties of Co-crystals

The allure of co-crystals is the possibility of attaining better physicochemical properties for troublesome compounds. The properties that are generally sought to be optimized are solubility, stability and bioavailability. Numerous studies have been performed to investigate these properties of co-crystals.[16-18]

1.3.1. Melting Point

The melting point of an API is related to its processability and stability. The numbers of studies that have been done on melting point changes induced by co-crystallization

are numerous. Aakeröy and co-workers[19] hypothesized that the melting point of an API may be tuned by co-crystallization. They went on to show that the melting points of five co-crystals – listed in Table 1 – of the anticancer agent hexamethylenebisacetamide (mp:181-182°C) were directly related to the melting point of the dicarboxylic acid co-formers (Table 1). In a different study, it was shown that the melting points of co-crystals were usually in between that of the co-former and the drug compound, or lower.[20] The observed trend is that co-crystallization does in almost all cases result in crystals that have melting points that are different from the melting point of the pure API. [1, 19, 20]

Table 1: Melting points of co-crystals and co-formers used in study by Aakeröy and co-workers.[19]

Co-former	Co-former melting point (°C)	Co-crystal melting point (°C)
Dodecanedioic acid	127-129	146-148
Sebacic acid	131-134.5	148-150
Suberic acid	141-144	158-160
Adipic acid	152.1	165-167
Succinic acid	184	186-188

1.3.2. Stability

There are studies that show that co-crystals can in some cases improve the stability of an API. Physical and chemical stability are important factors that highly influence the success of an API. Different types of solid state stability are investigated in the preclinical trial drug development. These include but are not limited to moisture sensitivity, air sensitivity and solution stability (the ability of co-crystal components to stay in solution and not precipitate out). The extreme moisture sensitivity of caffeine was improved by co-crystallization with oxalic acid.[21] The caffeine·oxalic acid co-crystal remained stable in 98% relative humidity for seven weeks whilst the caffeine crystal formed the hydrate soon after exposure to 98% relative humidity. Another example is the 1:1 co-crystal of saccharine and adefovir depivoxil, which proved to possess superior chemical stability when compared with the pure drug substance.[22, 23] The adefovir depivoxil·saccharine co-crystal stayed chemically stable for 29 days longer than the pure drug, which degraded to form mono-(pivaloyloxymethyl)-9-(2-phosphonylmethoxyethyl)adenine, pivalic acid and

formaldehyde when heated at 60°C. Other studies have been performed with a variety of co-crystals that have been subjected to different conditions including thermal,[16, 17] chemical,[17] solutions and thermodynamic stability.[18]

1.3.3. Solubility

Co-crystals have the ability to influence the lattice energy and the solvation of the crystal with varying degrees of success.[2] These two independent factors determine the solubility of the crystal. This makes the improvement of a drug's solubility using co-crystallization very plausible. Class 2 and class 4 drugs both have issues with solubility, thus improving solubility by co-crystallization is one of the key aims of many co-crystal screens.[4] In the case of the curcumin·resorcinol co-crystal, the solubility of the co-crystal was 4.7 times higher than that of the poorly soluble curcumin.[24] An even greater solubility increase by a factor of 11.8 was reported for the curcumin·pyrogallol co-crystal (Table 2).

Table 2: Amount of curcumin dissolved in 40% ethanol/water at 37°C over a period of 4 hours when starting from different solid-state forms.[24]

Compound	Amount dissolved (mg/L)
Pure curcumin	67.620
Curcumin·resorcinol co-crystal	111.025
Curcumin·pyrogallol co-crystal	179.609

There are many studies heralding the superiority of co-crystals and all the improvements that they can offer. Even though it is true that there are many cases of co-crystals enhancing the physicochemical properties of a drug compound, it must be noted that there are also cases where the co-crystallization has worsened the properties of the API. One such example is that of the carbamazepine co-crystals with highly soluble co-formers. These co-crystals were found to be more unstable in water because they quickly disintegrated to form the carbamazepine dihydrate.[25] So, even though co-crystallization can make things better it is not a one-size-fits-all solution for the issue of drugs with poor physicochemical properties.[4]

1.4. Designing Co-crystals: Crystal Engineering

Crystal engineering is a branch of crystallography that applies the knowledge of prevalent intermolecular interactions to design organic and organometallic crystal structures. Targeted attempts to design functional crystal structures using intermolecular interactions principles fall within the realm of crystal engineering, although these attempts may not always work out as planned. [26] Crystal engineering is the approach frequently used in co-former selection for co-crystal screening.[2] This is possible because pharmaceutical co-crystals are susceptible to design by crystal engineering since many APIs have multiple functional groups that can be used in crystal engineering endeavours.[8] These targeted functional groups can usually be used to form strong and directional intermolecular interactions. One such functional group is the carboxylic acid group, which was found in 30 of the top 100 selling prescription drugs in the United States of America.[27] This functional group is susceptible to hydrogen bonding and is often used in crystal engineering.

1.4.1. Intermolecular Interactions

There are many intermolecular interactions that play a crucial role in molecular recognition and molecular assembly.[27, 28] The two most important properties of intermolecular interactions are their strength and directionality. The strength of the interaction is important since that determines the quantity of influence which that particular interaction has on molecular assembly.[28] It must also be noted that with intermolecular interactions there is strength in numbers, i.e. numerous weaker interactions can outweigh the influence of stronger interactions. This is referred to as the Gulliver effect.[28] The second property is directionality. Interactions which are more directional are of greater significance because they can be exploited to achieve specific and pre-desired intermolecular orientations.

Non-directional (isotropic) intermolecular interactions are mainly of the dispersion and repulsion type.[28] These interactions are responsible for the close packing of molecules to form a crystal. Some of these interactions are C···C, H···H and ionic interactions. Directional (anisotropic) interactions have electronic distributions that give rise to certain chemical attributes.[28]

The most notable intermolecular interactions are hydrogen bonds, halogen bonds and charge transfer interactions.[8] Halogen atoms tend to interact with atoms that have lone pairs which results in an intermolecular interaction commonly known as the halogen bond.[29] Recently, halogen bonds have been under the spotlight because halogen bonds are of moderate strength and directionality which makes them a good intermediate between strong and weak hydrogen bonds.[30] The hydrogen bond is the most frequently used in supramolecular synthesis because it is a strong and directional interaction, making it ideal for influencing molecular assembly.[3]

1.4.2. The Hydrogen Bond

The IUPAC definition of a hydrogen bond is: "*an attractive interaction between a hydrogen atom from a molecule or a molecular fragment X–H in which X is more electronegative than H, and an atom or a group of atoms in the same or a different molecule, in which there is evidence of bond formation*." [31,32] Hydrogen bonds are represented as an interaction between a donor (D-H) and acceptor (A). The interaction is denoted with three dots between donor and acceptor (D-H···A). Characteristic features of the hydrogen bond – depicted in Figure 3 – are the hydrogen-acceptor distance (d) and the angle of the interaction $\angle$ D − H ··· A (θ). [33] For strong hydrogen bonding interactions, the strength of the interactions is in the range of 4 – 15 kcal mol^{-1} and the angle of the interaction tends toward 180°.[34]

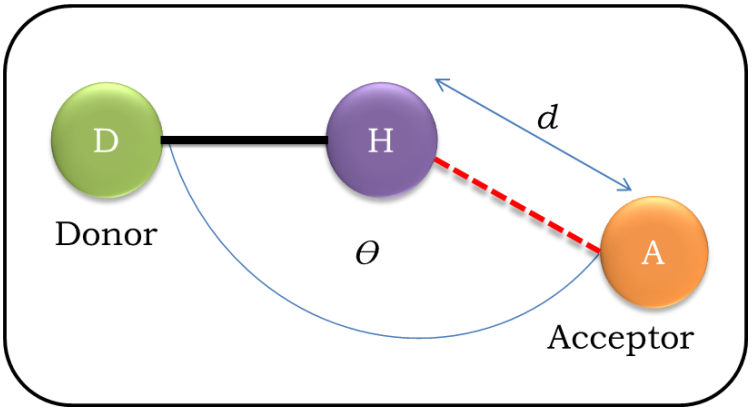

Figure 3: The hydrogen bond. The red dashed line indicates the intermolecular interaction and the black solid line a covalent bond. The interaction angle ($\angle$ D − H ··· A) is labelled as θ and the hydrogen··· acceptor (H···A) distance as *d*.

The standard "linear" hydrogen bond is shown in Figure 4a. In reality, the hydrogen bond angle is rarely 180° due to the spatial constraint of molecules. Also, the hydrogen can interact with a second acceptor (bifurcated hydrogen bond, Figure 4b). Very rarely is the hydrogen also seen to interact with three acceptors (trifurcated hydrogen bond, Figure 4c).[28] Multi-furcated interactions occur in organic crystals when there are more acceptors than donors.[28]

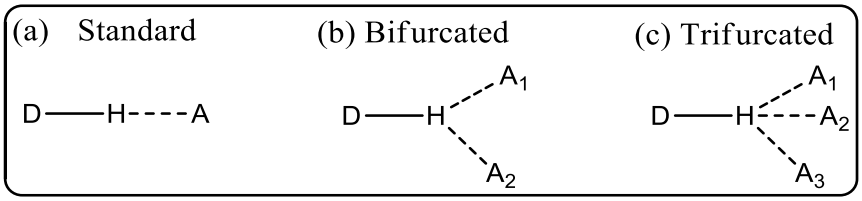

Figure 4: Different types of hydrogen bonding interactions. (a). The standard interaction with one acceptor. (b) Bifurcated interaction with two acceptors. (c) The trifurcated interaction with three acceptors.

The hydrogen bond is a cooperative interaction which is more stable when associated with other hydrogen bonds.[28] In other words, hydrogen bonds tend to aggregate in the form of dimers, trimers and chains.

1.4.3. Supramolecular Synthons and Retrosynthesis

Crystal engineering is synonymous with supramolecular synthesis. Supramolecular synthesis is analogous to covalent synthesis in organic chemistry (Figure 5). Just as atoms are held together by covalent bonds in covalent synthesis, molecules are connected by intermolecular interactions in supramolecular synthesis.

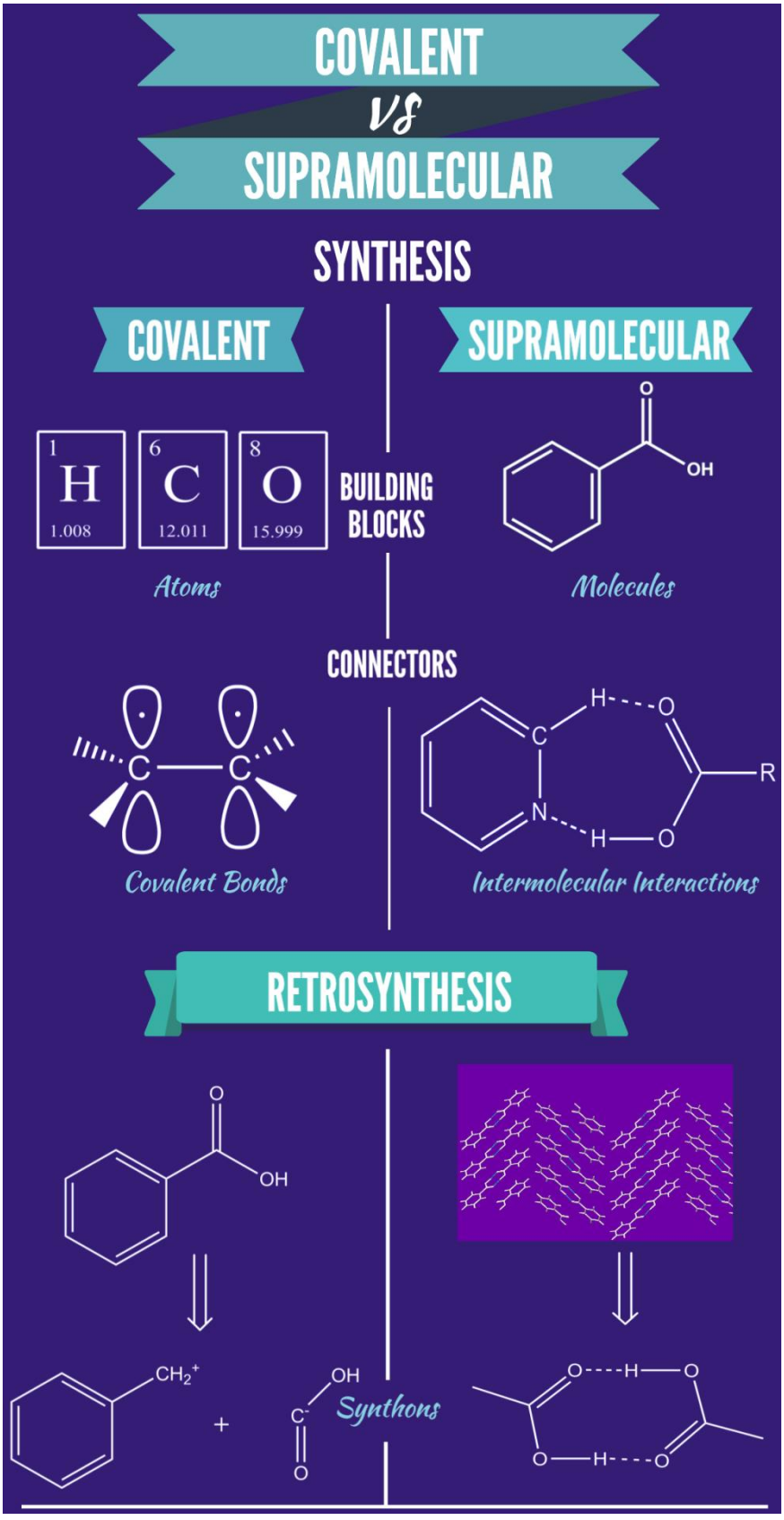

Figure 5: Infographic depicting supramolecular synthesis and covalent synthesis analogy.

In organic synthesis, the molecular synthons are *'small structural units within molecules which can be formed and/or assembled by known or conceivable synthetic operations'*[26] and so following from that in supramolecular synthesis, supramolecular synthons are *`structural units within supermolecules which can be formed and/or assembled by known or conceivable intermolecular interactions'.*[35] These structural units are spatial assemblies of intermolecular interactions between functional groups.[26] These supramolecular synthons (henceforth will be referred to only as synthons) make up the cornerstone of supramolecular synthesis.[28] Common synthons are functional groups cemented together with directional interactions such as hydrogen bonding (Scheme 1). However, not all synthons are held together by directional interactions. "Phenyl embraces" are patterns of triphenylmethanes and diphenylmethanes which are made up of C-H···C interactions.[28]

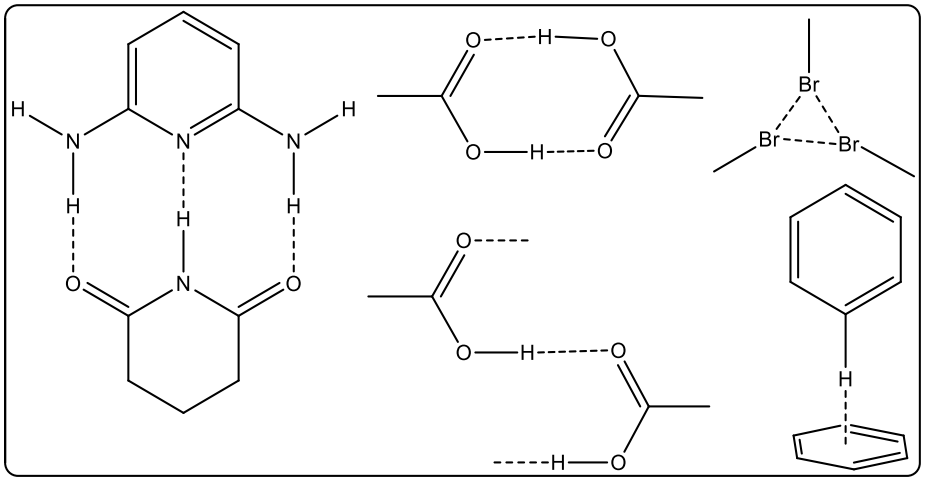

Scheme 1: Some representative supramolecular synthons.

Synthons have been classified as homosynthons or heterosynthons.[28] Homosynthons contain the same functional groups interacting with each other (Scheme 2a) and heterosynthons contain different functional groups interacting with each other (Scheme 2b).[28]

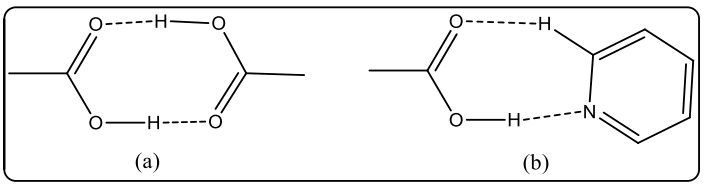

Scheme 2: Examples of a homosynthon and a heterosynthon. (a) Carboxylic acid homosynthon. (b) Carboxylic acid···pyridine heterosynthon.

The advantage of the synthon approach is that it provides a simplified way of understanding crystal structures. The approach also works best when useful synthons can be identified from known crystal structures.[26] These synthons can be identified by studying known crystal structures of molecules with similar structures or structural moieties. The disadvantage of the synthon approach is that, even though the formation of a particular synthon may be favourable, it may result in a supermolecule which cannot pack in an ordered crystalline fashion.[2] Moreover, the approach does not consider factors such as competition among the different functional groups present within the API or the co-former, nor does it consider the steric density around the donor and acceptor.[2]

1.5. Polymorphism

Polymorphism as defined by McCrone is "*a solid crystalline phase of a given compound resulting from the possibility of at least two different arrangements of the molecules of that compound in the solid state*" [36-39] This definition means that a given entity which can assemble in various patterns in the crystalline solid state is said to be polymorphic.

The high occurrence of polymorphism in APIs is attributed to their flexible structures.[40] In the study performed by SSCI, it was found that most of the compounds they screened for polymorphism exhibited polymorphic behaviour.[15] From the 245 compounds screened for polymorphism, it was found that 226 compounds had, at least, two or more polymorphs (Figure 6).

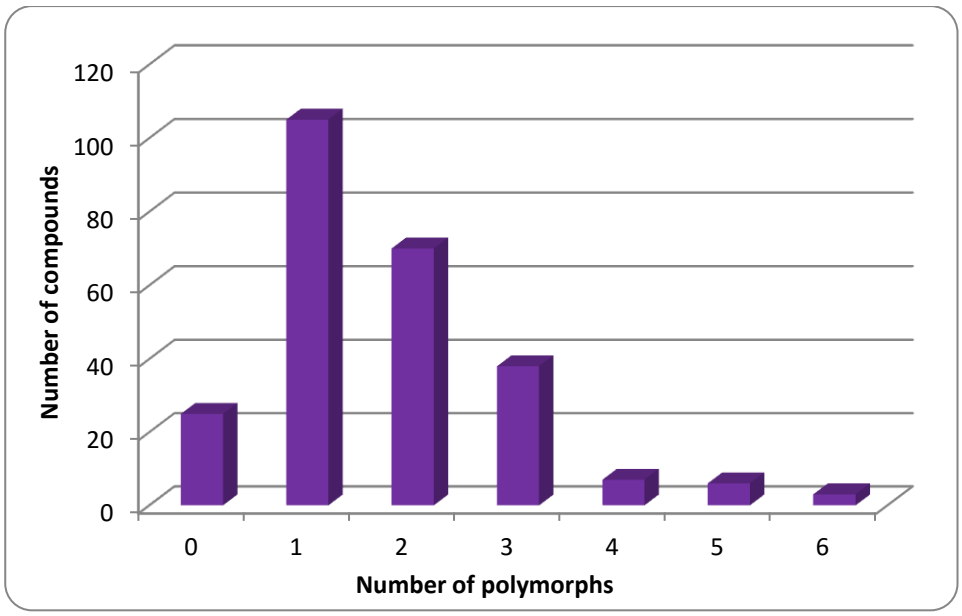

Figure 6: Plot showing the number of compounds that had one or more polymorphin a screen carried out on 245 compound by SSCI(Reproduced from Stahly).[15]

1.5.1. Thermodynamics

Polymorphs are categorized into two groups depending on the thermodynamic stability relationships between them.[38] The main approaches used to assess thermodynamic stability are based on Burger-Ramberger rules, and energy-temperature diagrams (Figure 7).[38] The Burger-Ramberger rules distinguish between the two categories which are monotropic and enantiotropic. The energy -temperature diagrams make the calculation of transition temperature possible. An enantiotropic relationship is one in which one polymorph is stable over a temperature range and undergoes a reversible transition into another form which is stable over a different temperature range.[41] Polymorphs are monotropically related when one polymorph is the most thermodynamically stable form from 0 K all the way up to its melting point, such that all other forms are metastable with respect to it.[42]

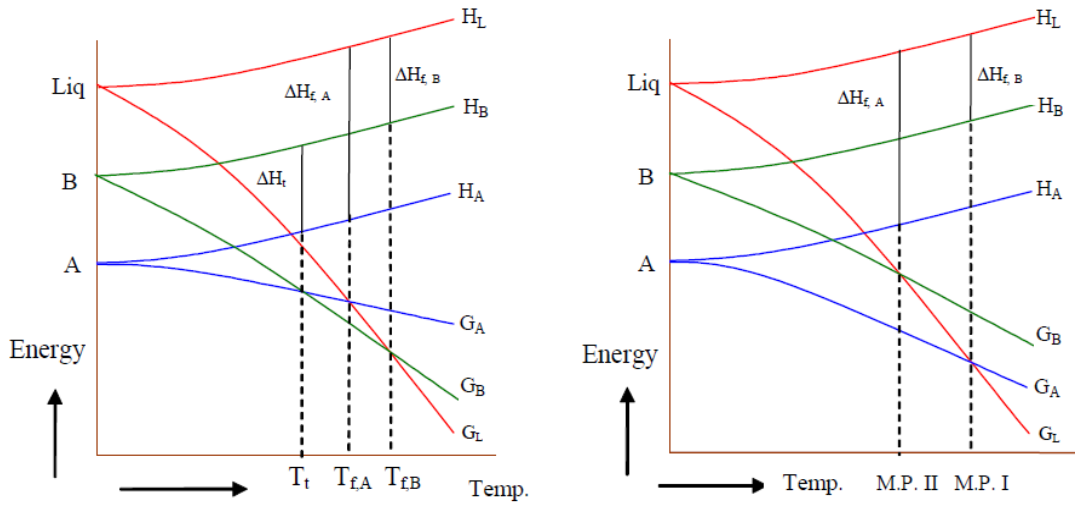

Figure 7: Energy-temperature diagrams for the enantiotropic (left) and monotropic (right) systems for solid phases of polymorphs A and B.[41]

1.5.2. Polymorphism in the Pharmaceutical Industry

It is estimated that 50% of drug molecules are polymorphic.[42] This is not surprising since pharmaceutical companies invest large sums of money and time in rigorous polymorph screens. Polymorphs of an API may have very different physicochemical properties this is the reason why screening for polymorphs is important in the pharmaceutical industry.[43] Abbott Laboratories discovered this the hard way when they lost an estimated $250 million in sales. This occurred when the commercial form of the drug Norvir had to be reformulated due to the crystallization of a then unknown polymorph of the API, ritanovir, and the new polymorph was not as active as the old one.[44]

1.5.3. Polymorphism in Co-crystals

Polymorphism is not only limited to single component systems. Co-crystals have exhibited polymorphism and various polymorphic co-crystals have been reported.[2] Literature is rife with studies investigating polymorphism of single component crystals.[45-46] In comparison, reports on polymorphism in co-crystals are not as ubiquitous.[47] Polymorphism in co-crystals (Figure 8) presents an expansion of the optimization space around a pharmaceutical compound and also offers the opportunity to develop novel patentable material.[2] The number of reported

polymorphic co-crystals has increased in recent years.[40] Additionally, advances in experimental techniques have made polymorph screening less of a serendipity-dependent affair and have paved the way for more successful screens.[48]

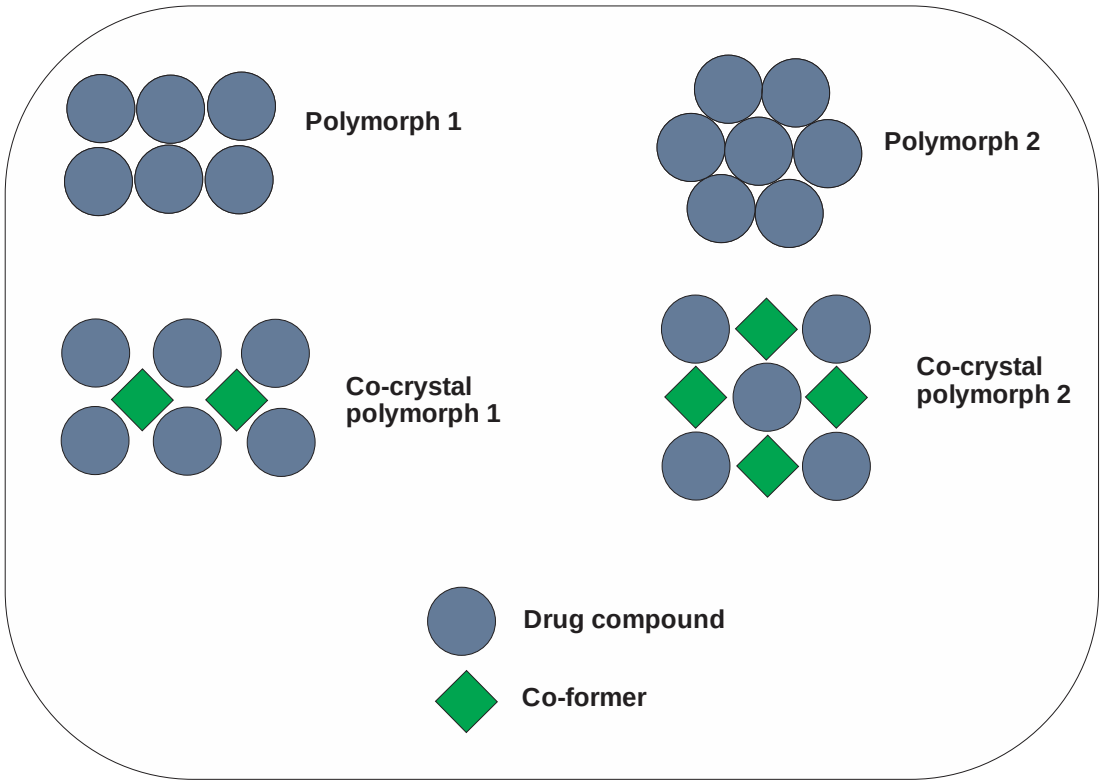

Figure 8: Diagrammatic representation of polymorphs in single and multi-component crystals.

1.5.4. Classification of Co-crystal Polymorphs

In single-component crystals, the key intermolecular interactions are usually retained in different polymorphs. For compounds with significant conformational changes between polymorphs, the designator conformational polymorphs is used.[38] In cases with different packing yet similar conformations of molecules, the polymorphs are called packing polymorphs.[38] Most often both packing and conformational changes are observed between polymorphs.[49] Co-crystals contain two or more molecules in the crystal so considering only packing and conformational changes in order to classify polymorphs would not suffice, intermolecular interaction contributions also need to be considered.[40] These classifications are not used in the strictest sense and polymorphs can belong to more than one class. Nonetheless, the

classification system is useful in making the nature of polymorphism easy to identify and quantify.

Synthon polymorphism

Synthon polymorphs have different primary intermolecular interactions. Molecules that contain multiple hydrogen bonding capabilities appear to be more prone to form synthon polymorphs[40]. Co-crystals with different hydrogen bonding patterns have been reported. An example is the polymorphic co-crystals of 2,3,5,6-tetramethylpyrazine and 4-hydroxybenzoic acid. Form **I** of this crystal contains acid–acid dimer and hydroxyl–pyridine heterosynthon; Form **II** has acid–pyridine and hydroxyl–carbonyl heterosynthons (Figure 9).[50]

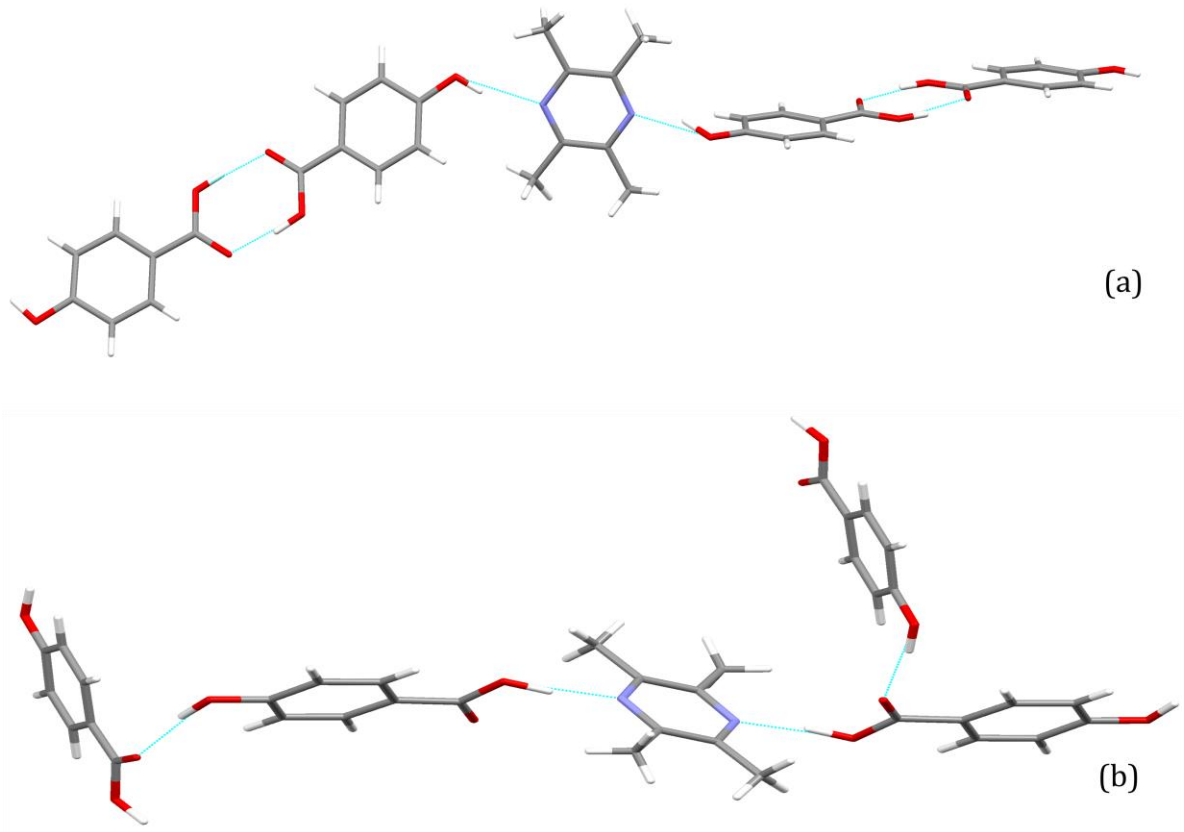

Figure 9: Synthon polymorphism in 2,3,5,6-tetramethylpyrazine and 4-hydroxybenzoic acid co-crystals.[50] (a) Hydrogen bonding patterns observed in Form I of the co-crystal. (b) Hydrogen bonding patterns observed in Form II of the co-crystal.

Conformational Polymorphism

Conformational polymorphism arises when flexible molecules are present in a co-crystal. This tendency to form polymorphs stems from significant changes in the conformation of one (or more) of the molecules in the co-crystal. According to Aitipamula *et. al.*[40] conformational polymorphism is more common than synthon polymorphism, thus, flexible molecules are adding to the diversity of polymorphism in co-crystals.

Tautomeric polymorphism

Tautomeric polymorphs occur when different tautomers crystallize in different crystal forms. Tautomers that interconvert in solution or melt are considered the same, so co-crystals containing those different tautomers are considered polymorphs.[40] This type of polymorphism is rare. An example of tautomeric polymorphism is observed in the co-crystal of piroxicam and 4-hydroxybenzoic acid, which has two tautomeric polymorphs.[51] In the one polymorph piroxicam is present in its non-ionized state and in the other the zwitterionic form is present.

Packing polymorphism

Packing polymorphism is when the overall 3D arrangement is different in polymorphs. Packing polymorphism is more common in co-crystals containing completely rigid molecules or molecules with weak conformational flexibility.[40] A textbook example of packing polymorphism is the 2:1 polymorphic co-crystal of 2-aminopyrimidine and benzoic acid.[52] With both molecules being rigid, the possibility of conformational polymorphism is low. The same intermolecular interactions are present in both crystals. The difference between the two polymorphs is only the packing. In Form **I** there is a herringbone packing arrangement (Figure 10a) whereas Form **II** does not contain the herringbone arrangement (Figure 10b).

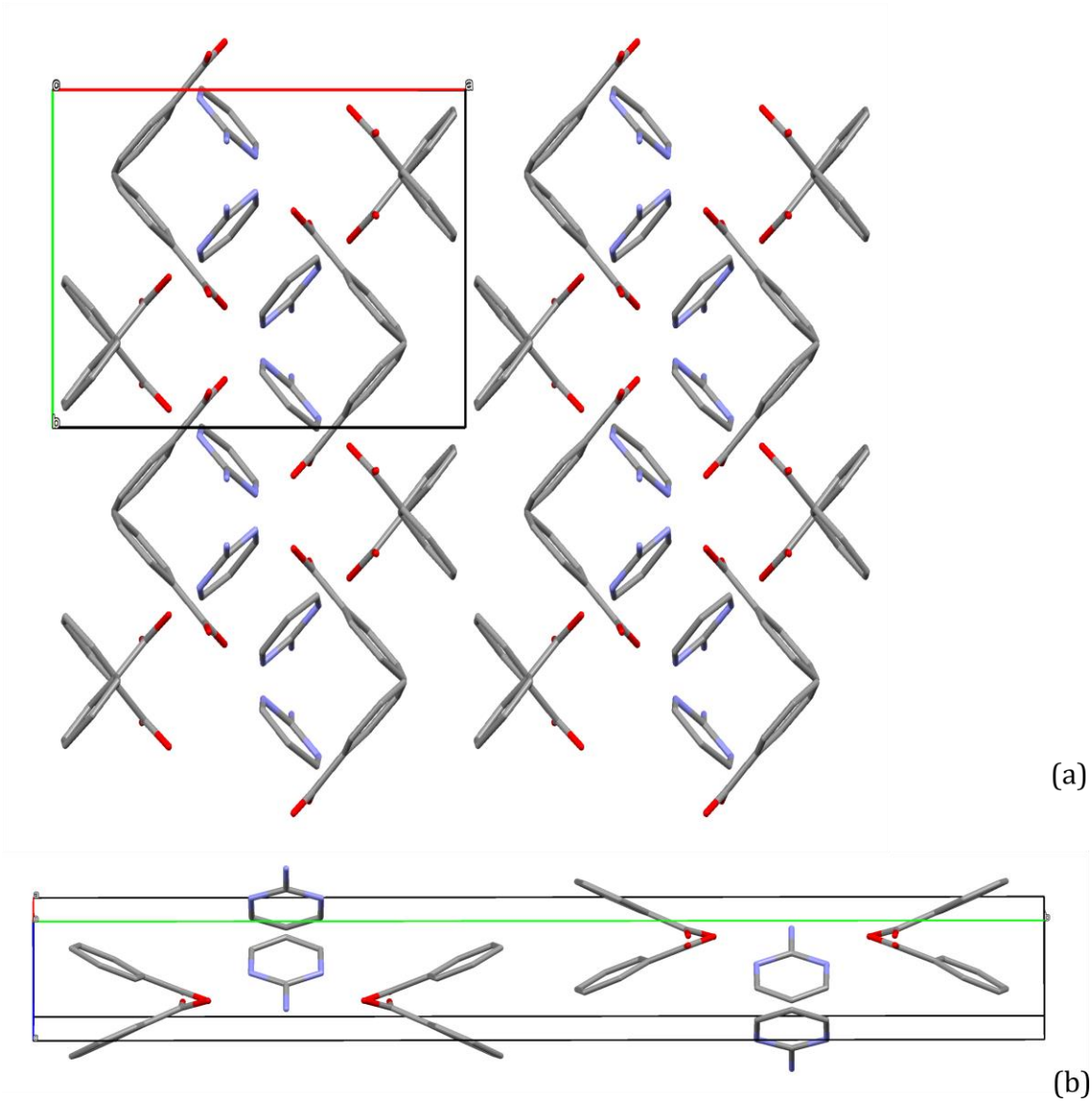

Figure 10: Packing polymorphism observed in polymorphic co-crystal of 2-aminopyrimidine·benzoic acid. (a). Form I of 2-aminopyrimidine·benzoic acid co-crystal. (b) Form II of 2-aminopyrimidine·benzoic acid co-crystal.

1.6. The Cambridge Structural Database

In supramolecular retrosynthesis the synthons which are observed in known crystal structures are the ones to be relied on most frequently because of the probability of them forming in the target supermolecule is high.[13] Supramolecular synthesis is based on the understanding and manipulation of robust synthons; however, in order to know which of these synthons are indeed robust, a representative collection of crystal structure data is required.[13] The Cambridge Structural Database (CSD)[53] fulfils

the role of housing such data.[13] The CSD is a depository for X-ray and neutron data on organic and organometallic crystals created by the Cambridge Crystallographic Data Centre. Currently, the database holds over 800 000 structures (November 2015). This database is the ideal place to gain an understanding of the frequency and kinds of polymorphism found in co-crystals. Even though not all reported organic crystal structures are deposited into the database, a good approximation of the propensity of polymorphism in small molecule organic co-crystals may still be obtained.

1.7. Aims

The goal of this project was to screen for polymorphic co-crystals from a pool of known co-crystals. This is important because there is a gross lack of data regarding polymorphism in co-crystals. Since co-crystals present a new paradigm in the realm of optimisation of pharmaceuticals, it is imperative that co-crystals and their behaviour are well understood.

The objectives of this MSc project are to:

- Perform a database survey;
- Screen for polymorphs of selected co-crystals;
- Isolate and characterize the polymorphs that are found.

2. The Hunt for Polymorphic Co-Crystals

2.1. Introduction

Recent reports by Aitipumula and co-workers found that as of September 2013 there were 114 polymorphic co-crystals reported in the literature.[40] In an earlier study,[54] the group reported that an "exhaustive" analysis of the CSD showed that the percentage of polymorphic co-crystals is comparable to the percentage of polymorphic single component crystals. In the same year (2010), Zaworotko *et. al.* [55] reported a similar observation in their published database analysis.

A database analysis of the co-crystal structures deposited in the CSD was performed. The analysis was performed in order to find out how many polymorphic co-crystals are currently in the CSD and how many of those are pharmaceutical co-crystals.

2.2. Methodology

Searches were performed in the CSD[53] (version 5.36 with the November 2014, February 2015 and May 2015 updates) using *ConQuest*(version 1.17).[56] Structures were visualised using *Mercury* (version 3.5).[56, 57]

Binary organic co-crystals which fall into the definition mentioned in Chapter 1 were isolated. In order to narrow the scope of the analysis, the following restrictions were imposed.

i. Organic co-crystals containing only C, H, O, N, S, F, Cl, Br, and I were targeted.
ii. Molecules must be solid at standard temperature and pressure.
iii. Crystals containing zwitterions were excluded.
iv. Clathrates and inclusion complexes were excluded.

Figure 11 shows the queries and Boolean logic used to search for hits that satisfy the aforementioned search parameters. Query one was used get hits that contain two

different compounds in the crystal. Query two ensures that the structures have at least one hydrogen and an oxygen atom and between five and forty carbon atoms. Queries two and three are used to obtain hits that contain the elements C, H, O, N, S, F, Cl, Br, I only. Zwitterions were excluded by searching for structures that did not contain any charge on any atom (query four). Due to earlier searches that yielded a large number of hits that contained common solvent and gas molecules but were not identified as solvates an additional restriction on the formula was added. None of the individual molecules in the structure could have fewer than five carbon atoms (query five). Furthermore, stray solvates were removed manually. Queries six to eight eliminated the hydrates, clathrates and solvates respectively. Hits were subjected to additional filters that ensured that hit had:

- 3D coordinates determined;
- no ions;
- no powder structures;
- not polymeric;
- no errors.

Crystal structures in the CSD are grouped according to chemical entities in the structure. A group of structures contain the same entities is assigned a 'refcode' which is made up of six letters. The individual entries are indicated by the addition of two numbers at the end of the refcode. Polymorphic crystal structures are placed in the same refcode family with a small number of assignment errors.[i] Polymorphs were isolated by searching the dataset for structures flagged as polymorphs. Additionally, manual analysis of refcode families and the dataset was conducted to isolate the co-crystals that are not flagged as polymorphs. The isolated polymorphs were then classified according to the type of polymorphism. Duplicate structures and stray solvates were removed manually.

Pharmaceutical co-crystals were identified and isolated in two ways. The first approach was to search the dataset for crystal structures that contained either the

[i] Two examples of this error were found for the polymorphic co-crystals of (6-methoxy-1,3-benzothiazol-2-amine) and decanedioic acid (FEXHOH and UYAZEA) and the co-crystals of salicylic acid and 4,4'-bipyridine (KONZEU and KOPKEH).

word “drug” or “pharmaceutical” in the crystal description. The remaining pharmaceuticals were identified manually be online searches for the individual molecules within the crystal or the common names of the molecules if given.

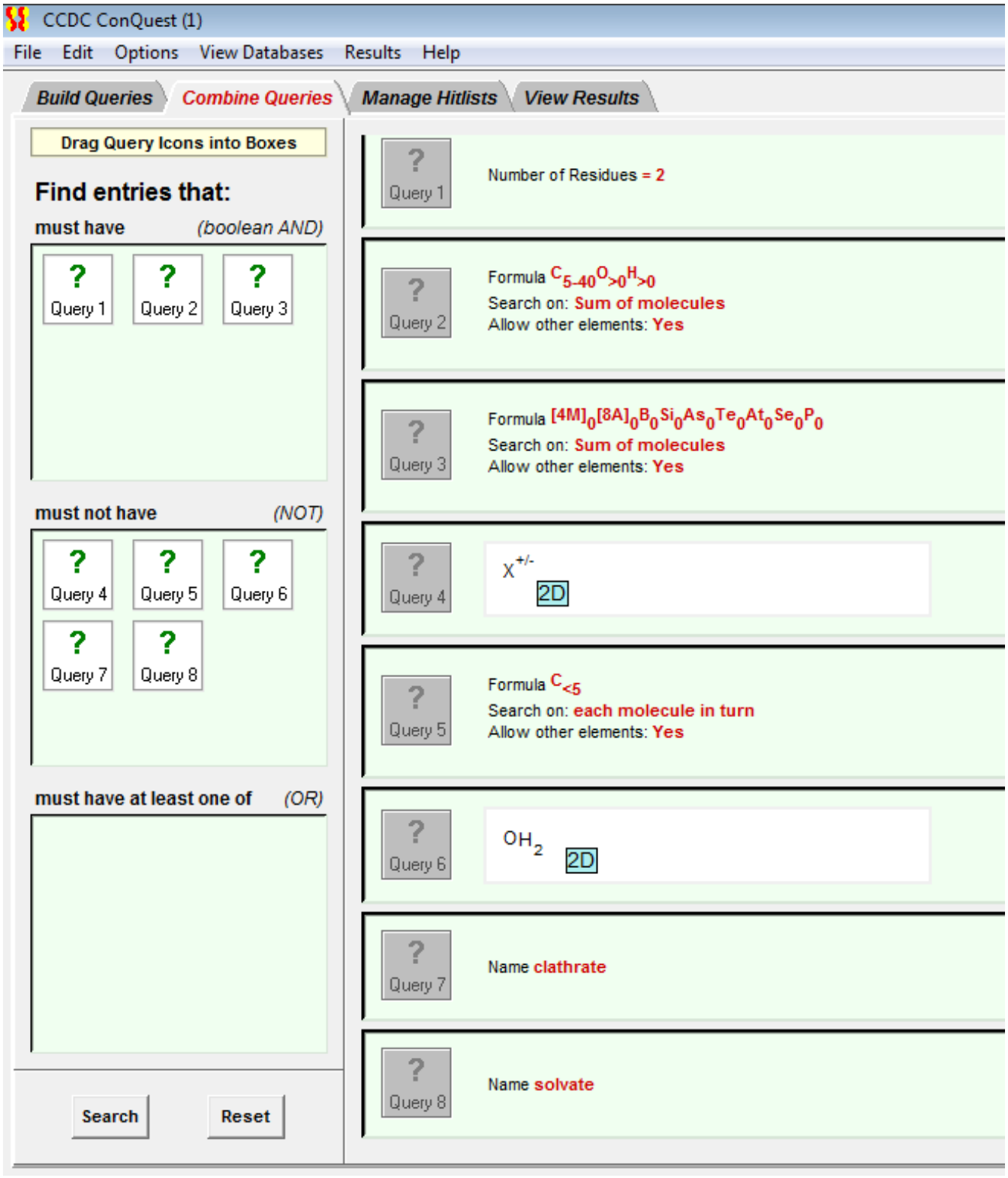

Figure 11: Screenshot of *ConQuest* showing the queries and Boolean logic used to generate the hit list for database survey.

2.3. Results

There was a total of 2925 neutral organic co-crystals found in the CSD. There were 400 pharmaceutical co-crystals and 239 polymorphic co-crystals within the 2925 hits (Figure 12). The polymorphic co-crystals were categorized according to the type of polymorphism. The co-formers of the pharmaceutical co-crystals were analysed and grouped according to whether they were GRAS, non-GRAS or a second drug compound. As is true for any data survey, there may be inadvertent omissions due to oversight; we present our apologies to the authors of those articles.

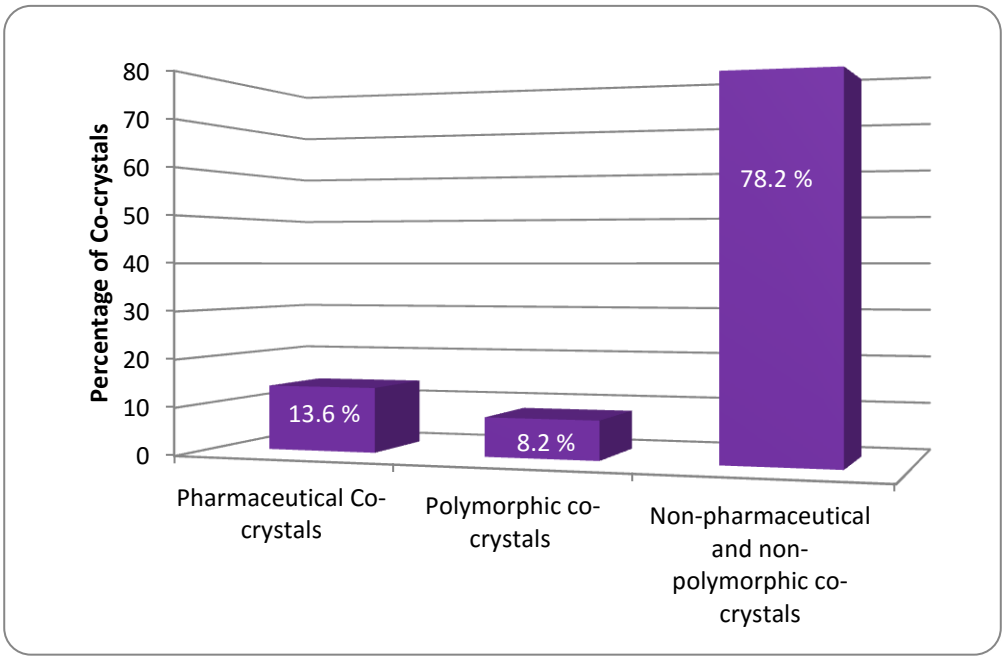

Figure 12: Plot showing the propensity of pharmaceutical co-crystal and polymorphs in co-crystals in a CSD study of 2925 neutral organic co-crystals.

2.3.1. Polymorphic Co-crystals

How prone co-crystals are to polymorphism is a question that many groups have tried to address, but up to now there is insufficient data available on polymorphic co-crystals to be able to draw a conclusion.[40] This study attempts to address this by categorizing the currently available data on polymorphic co-crystal in order to get an overview of what kinds of polymorphism are prevalent in co-crystals.

The search performed found 239 polymorphic co-crystals. These co-crystals had an almost even distribution of synthon, packing and conformational polymorphism (Figure 13). None of the co-crystal showed tautomeric polymorphism. The case of piroxicam was not included due to the fact that in one of its polymorphs crystallized as a zwitterion.

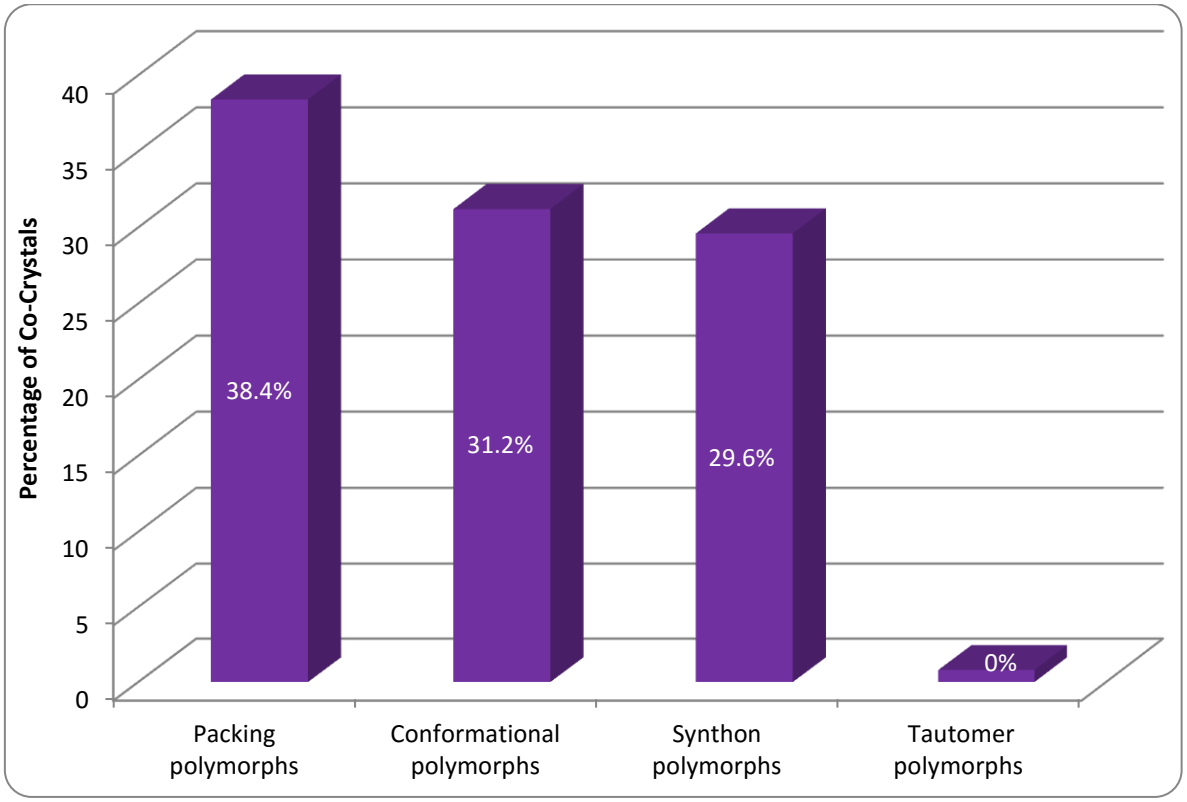

Figure 13: Plot showing percentage of co-crystals that exhibited various types of polymorphism in a CSD screen of 239 polymorphic co-crystals.

Packing and conformational polymorphs were the two highest types of polymorphism. In the packing polymorphism group, all the co-crystals had similar intermolecular interactions and the molecules had similar conformations. The only change was the packing in the different polymorphs. For example, the co-crystal of *N*,*N*'-diacetylpiperazine and 2-hydroxybenzoic acid had $O\text{-}H_{(carboxylic\ acid)}\cdots O{=}C_{(amide)}$ heterosynthons between the piperazine and benzoic acid in both polymorphs.[52] Also both molecules are relatively rigid and the conformations of the molecules in the polymorphs are similar. The only difference between the two polymorphs is their

packing, which in form **I** has a zigzag-like pattern (Figure 14a), and in form **II** has two-dimensional layers of each co-former (Figure 14b).

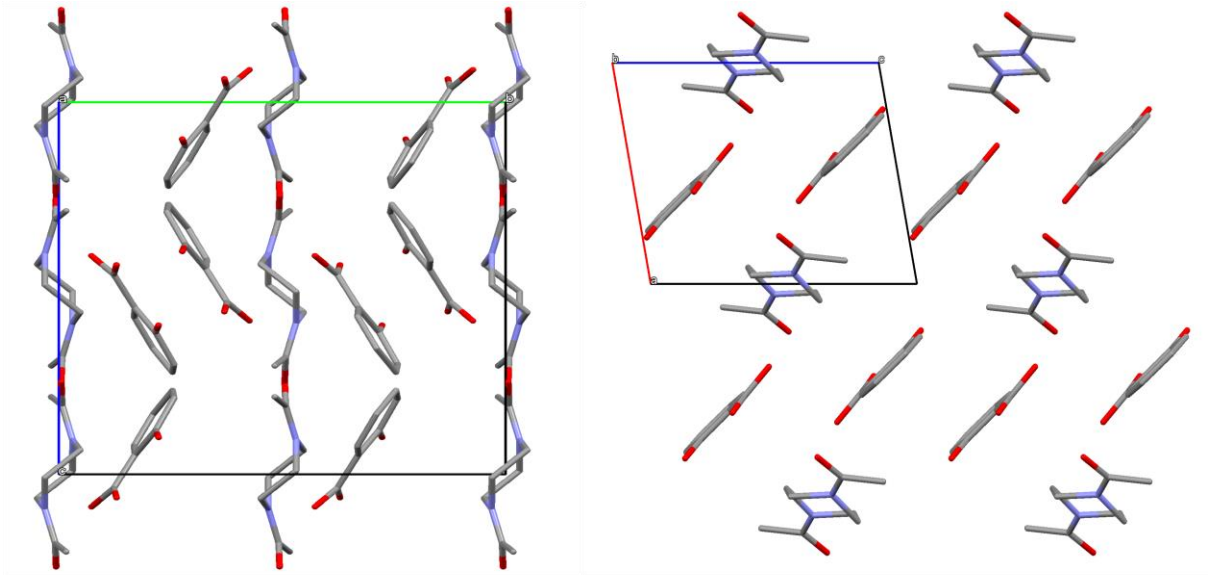

Figure 14: The packing in the polymorphic co-crystals of *N,N'*-diacetylpiperzine and 2-hydroxybenzoic acid.[52](a)Packing diagram of form I of the co-crystal. (b) Packing diagram of form II of the co-crystal.

As noted by Aitipamula *et. al.* conformational polymorphism is more common than synthon polymorphism,[40] although the gap between the two is not large, with 32% of co-crystals having conformational polymorphism and 30% having synthon polymorphism. The flexibility of compounds such as AMG 517 and 1,2-bis(4-pyridyl)ethane can be seen in their co-crystalline solid states, in which these compounds have polymorphic co-crystals which contain different conformations of the compound. Figure 15 shows overlays of the molecules in some co-crystals that exhibit conformational polymorphism.

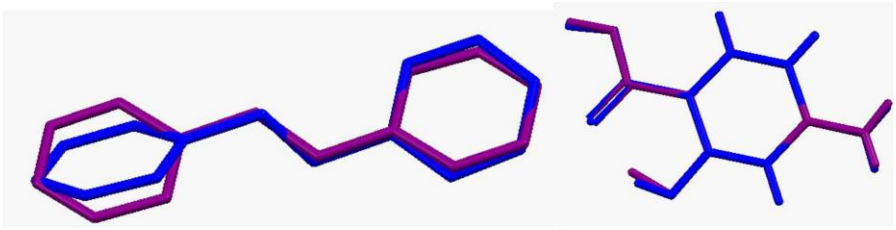

p-Aminosalicylic acid·1,2-bis(4-pyridyl)ethane

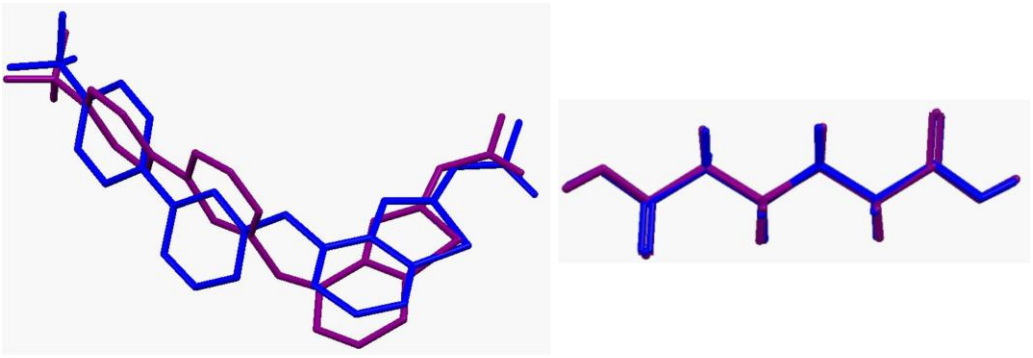

AMG 517·adpic acid

Figure 15: Some examples of conformational polymorphism.[58, 59] The molecules in purple are from form I of the different co-crystals and the molecules in blue are from form II of the different co-crystals. Changes in conformation are observed in the molecules on the left and these changes then result in the different polymorphs of the co-crystal.

There were multiple co-crystals that displayed synthon polymorphism. In total 39 pairs of co-crystals were found to be related by synthon polymorphism. One such example is the co-crystal of 4,4'-bipyridine and 4-hydroxybenzoic acid.[60] In form **I** polymorphs there are carboxylic acid dimers which interact with the 4,4'-bipyridine via a hydroxy···pyridine interaction (Figure 16a). In polymorph **II,** the carboxylic acid dimer is not present and the co-crystal is sustained by a pyridine···carboxylic acid heterosynthon and a hydroxy···carboxylic acid interaction (Figure 16b).

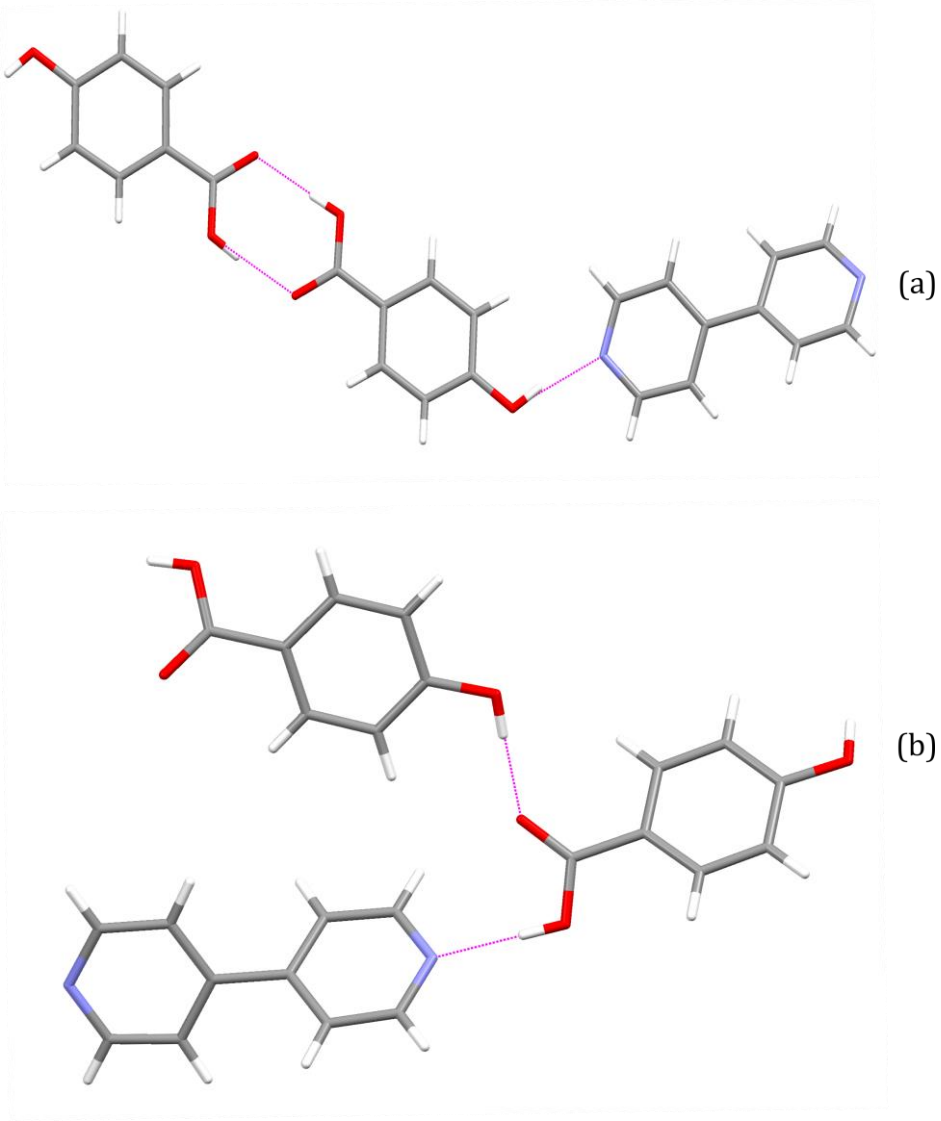

Figure 16: Synthon polymorphism in co-crystal of 4-hydroxybenzoic acid and 4,4'-bipyridine.[60](a) Hydrogen bonding synthons observed in form I of 4-hydroxybenzoic acid·4,4'-bipyridine. (b) Hydrogen bonding synthons observed in form II of 4-hydroxybenzoic acid·4,4'-bipyridine.

2.3.2. Pharmaceutical Co-crystals

With a large amount of interest in pharmaceutical co-crystal in recent years, a survey of the CSD was performed in order to gauge the amount of data contributed by co-crystals screens of API. The total number of pharmaceutical co-crystals found in the CSD was 400, which is 14% of the total number of neutral co-crystals. This percentage is very low and is most likely not a true reflection of the situation. This is

because many drug compounds have zwitterionic forms and many of the screens performed in industry are not deposited into the database.

The types of co-formers used for the co-crystallization of these pharmaceutical co-crystals were assessed. It was found that most of the co-formers used were non-GRAS compounds and only 47% (including drug-drug co-crystals) were GRAS compounds. It was also found that there were a significant number of drug-drug co-crystals (co-crystals composed of two or more drug APIs) (Figure 17). Of the 400 pharmaceutical co-crystals, 145 were co-crystals with GRAS co-formers and 44 were drug-drug co-crystals.

There were 56 pharmaceutical co-crystals which were found to be polymorphic. In the co-crystals found in the CSD, caffeine proved to be the API with the highest number of polymorphic co-crystals (5). Figure 18 lists the co-formers used in the five polymorphic co-crystals of caffeine and also the type of polymorphism.

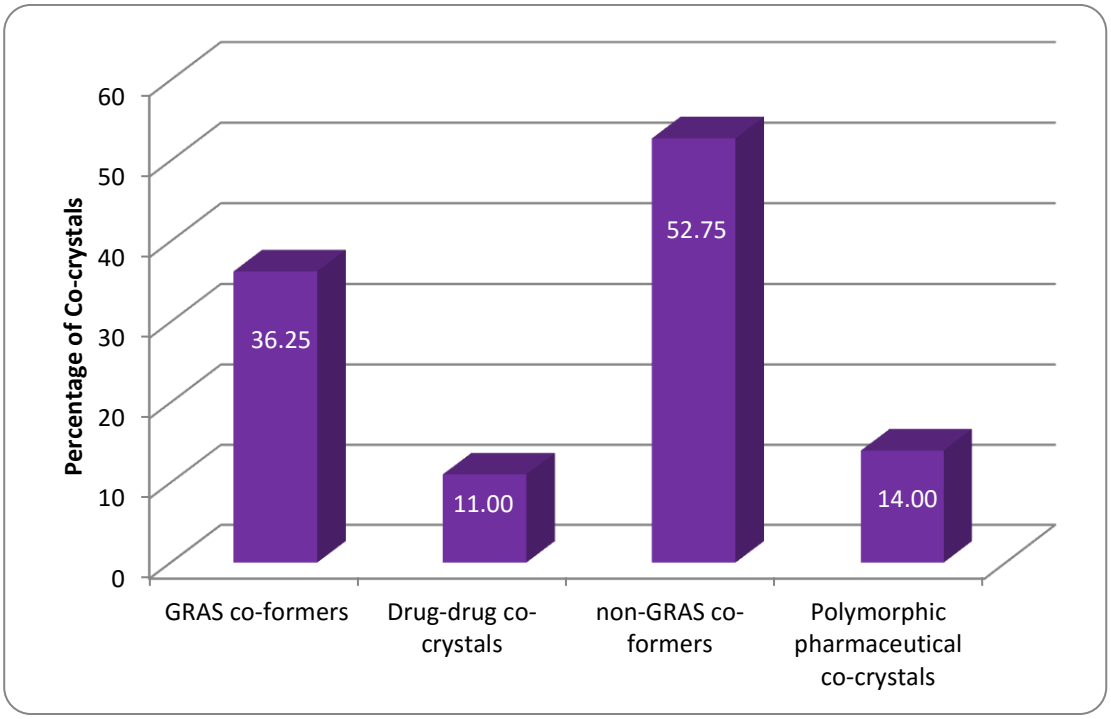

Figure 17: Plot showing the percentage of co-crystals that fell into different types of pharmaceutical co-crystal groups in a screen carried out on 400 pharmaceutical co-crystals found in the CSD.

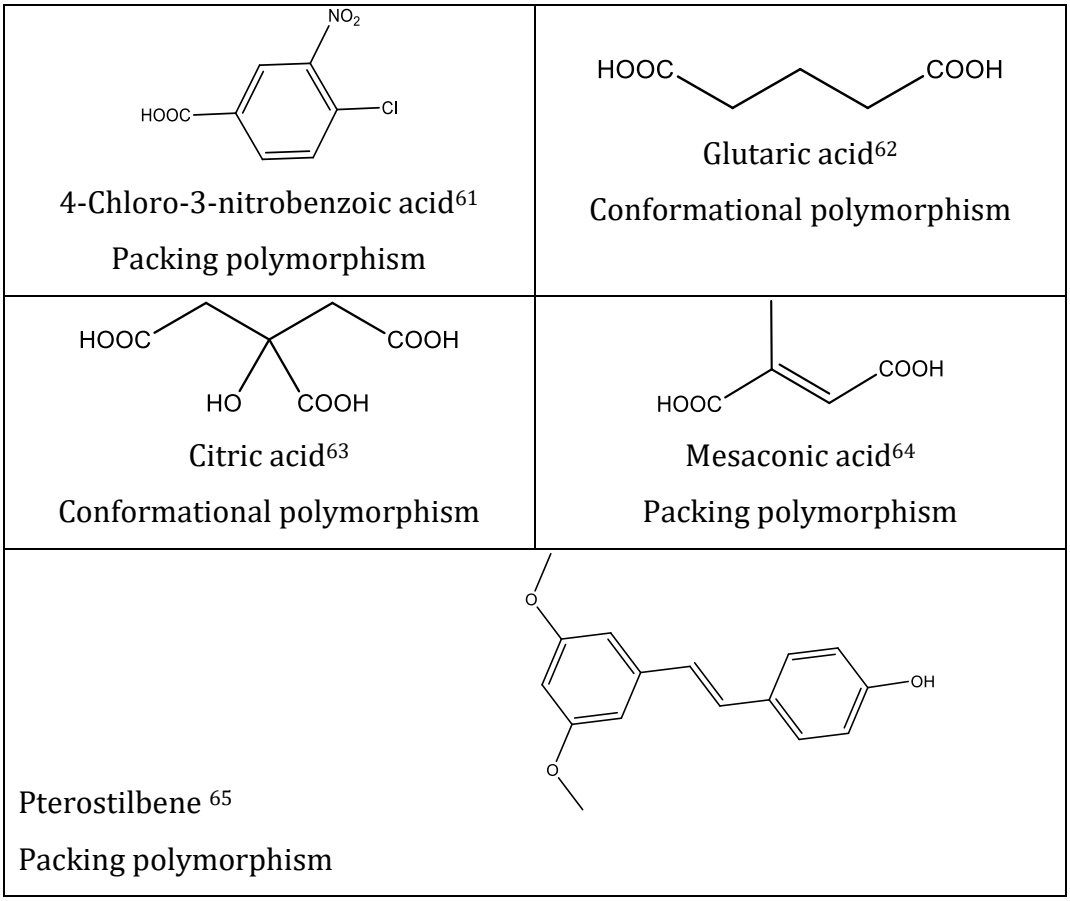

Figure 18: The different co-formers found in the 5 polymorphic caffeine co-crystals and the type of polymorphism observed in each co-crystal.

3. Methods and Materials

There are many methods of crystallization available to one seeking to grow crystals. Which methods will be successful is system dependent and as a result it is common place in the realm of crystal growing to try multiple methods in order to obtain the desired crystal structure. When screening for polymorphs it is even more so important to expose the system to different crystallization because this increases ones chances of success, for this reason, many crystallization experiments were performed using different conditions.

Due to the high volume of experiments performed this chapter gives a brief overview of the key methods employed during the study and a more detailed account of the experiments performed - including solvents, temperatures, and crystallization methods used - is given in digital appendix B The different APIs and co-formers used in the study are listed in Table 3.

Table 3: List of the active pharmaceutical ingredients used in the project along with the co-formers used for the polymorphism screen.

Active pharmaceutical ingredient	Co-formers
Theophylline	3,4-dihydroxybenzoic acid 3,5-dihydroxybenzoic acid 2,5-dihydorxybenzoic acid 2,4-dihydroxybenzoic acid Cinnamic acid
Carbamazepine	Cinnamic acid
Piracetam	L-Tartaric acid Mandelic acid Glutaric acid Citric acid
Flufenamic acid Mefenamic acid Tolfenamic acid.	4-Aminopyridine 3-Aminopyridine 2-Aminopyridine 2-Amino-3-bromopyridine 2-Amino-5-bromopyridine 2-Amino-5-chloropyrine 2-Amino-3-hydroxypyridine 2-Amino-3-nitropyridine 2-Amino-5-nitropyridine
Furosemide	Caffeine 4-Aminobenzoic acid Nicotinamide Isonicotinamide

3.1. Polymorph Screening Techniques

The screen for polymorphs began with known pharmaceutical co-crystals. The co-crystals were subjected to a series of polymorph screening exercises. The polymorph

screens involved altering the environmental conditions of the crystallization process in order to encourage the growth of different polymorphs of the co-crystals.

3.1.1. Slow Evaporation

In this method, the API and co-former were dissolved in a solvent (or mixture of solvents) and the solvent was allowed to evaporate off slowly in order to induce crystal growth. By altering the solvent, temperature and saturation different polymorphs may be grown from solution.

3.1.2. Slow cooling

In this technique, the API and co-former were dissolved in a solvent to form a supersaturated solution. The solution was heated up and linearly cooled to room temperature over a number of days. The cooling was performed in an oil bath which was placed on a hot plate connected to a thermocouple which adjusted the temperature as required in order to ensure the sample cooled down slowly. By cooling the solution slowly the system was subjected to different nucleation environments in which different molecular assemblies could be stable long enough to form new polymorphs.

3.1.3. Solvent-Assisted Grinding

In this method, the API and co-former were ground together with a few drops of solvent for a period of time. The grinding was performed in a pestle and mortar. The starting materials were ground with the drop-wise addition of various solvents. A mixer mill was also used for grinding experiments. The instrument used was a Retsch MM200 mixer mill. It was used with stainless steel canisters and two stainless steel balls per canister.

3.1.4. Heterogeneous Seeding

Matzger and co-workers[66-69] have shown that using different polymers as heterogeneous seeds can lead to the discovery of different polymorphs of both single and multiple component systems. This method was employed by adding different kinds of polymers to saturated solutions and crystals were grown on the polymers as

the solvent evaporated (Figure 19). The polymers used were nylon 6/10, nylon 6/6, nylon 11, nylon 12 and polyethylene.

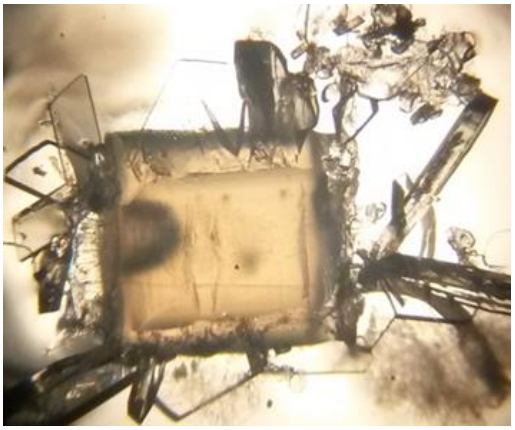

Figure 19: Single crystals of 3,4-dihydroxybenzoic acid (form I) growing on a polyethylene bead.

3.2. Instrumentation

3.2.1. Single Crystal X-Ray Diffraction (SXRD)

Single crystal x-ray diffraction (SXRD) was used to obtain the 3D structure of a crystalline material. The diffractometer uses a Bruker APEX II CCD area detector and graphite monochromated MoKα_1 radiation (50kV, 30mA) to collect the diffraction data. The data collections were performed at -100°C. *SAINT+*[70] was used to perform the data reduction. Absorption corrections and space group assignments were done using *SADABS*[71, 72] and *XPREP* [70]respectively.

Crystal structures were solved and refined using *SHELXS-97*[73, 74] on the *WinGX* suite.[75] *SHELXS-97* used direct methods to solve the crystal structure and refinements were done using full-matrix least-squares/difference Fourier techniques on F^2. All non-hydrogen atoms were refined anisotropically. All hydrogen atoms were placed in calculated positions with aromatic C-H = 0.95 Å, hydroxyl O-H = 0.84 Å or amine N-H = 0.88 Å and U_{iso} (H) = 1.2U_{eq} (C), U_{iso} (H) = 1.5U_{eq}(O) and U_{iso} (H) = 1.2U_{eq}(N). Diagrams were generated using *ORTEP-3*[75], *PLATON* [76] and *DIAMOND* [77].

3.2.2. Powder X-Ray Diffraction (PXRD)

Powder X-Ray Diffraction (PXRD) patterns were collected at 293 K on a Bruker D2 Phaser diffractometer which utilizes a sealed tube Co X-ray source (λ = 1.78897 Å), operating at 30 kV and 10 mA, and LynxEye PSD detector in Bragg-Brentano geometry.

3.2.3. Differential Scanning Calorimetry (DSC)

Differential Scanning Calorimetry (DSC) was performed on a Mettler Toledo DSC822^{e} using sealed aluminium pans under air. The machine was calibrated using indium with a purity of 99.99%, a melting point of 156.6^{o}C and heat of fusion 28.45 J g^{-1}. Various heating and cooling programs were be used in order to gather information regarding the melting point, enthalpy of melting for various screening methods. STAR-SW 9.20 was used for instrument control and data analysis.

3.2.4. Hot Stage Microscopy (HSM)

The hot stage was used is a Kofler Hot Stage placed upon an Olympus SZ61 microscope. This technique was used to observe phase transitions and photograph them.

4. Co-Crystals of Theophylline

Theophylline (TPL) is a drug used in the treatment of respiratory diseases such chronic obstructive pulmonary disease and asthma.[78] It is part of the xanthine family and is an analogue of caffeine and theobromine.[78] Some co-crystals of theophylline have been shown to drastically enhance the properties of theophylline.[62]

4.1. Synthon Competition in Co-crystals of Theophylline

Theophylline has various possible hydrogen bond donors and acceptors. This opens it up to the possibility of various hydrogen bonding frameworks within its crystals and this also contributes to making theophylline polymorphic. Within the three polymorphs of theophylline for which crystal data are available, three of the four different hydrogen bonding motifs are observed (Scheme 3). In Form **I** [79, 80] the observed hydrogen bonding motif is a discrete interaction between the $N\text{-}H_{(imidazole)}$ and the $O{=}C_{(urea)}$ (Scheme 3a). Form **II** [80, 81] display a **C(4)** chain motif formed by the $N\text{-}H_{(imidazole)}$ and the $N{=}C_{(imidazole)}$ (Scheme 3b). Form **IV** [79, 82] is stabilised by the formation of a ring consisting of two $N\text{-}H_{(imidazole)}\cdots O{=}C_{(amide)}$ interactions (Scheme 3c).

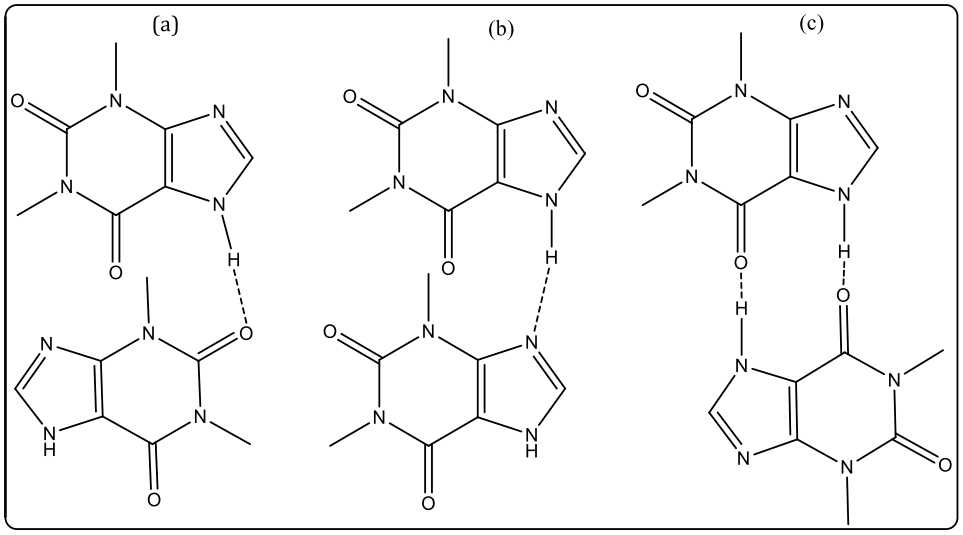

Scheme 3: Hydrogen bonding motifs observed in the three reported polymorphs of theophylline: (a) Form I: N-$H_{(imidazole)}$···O=$C_{(urea)}$ heterosynthon, (b) Form II: N-$H_{(imidazole)}$···$N_{(imidazole)}$ heterosynthon (c) Form IV: N-$H_{(imidazole)}$···O=$C_{(amide)}$ dimer homosynthon.

Theophylline's preference for different hydrogen bonding motifs is also observed in its co-crystals. In its co-crystals with various dihydroxybenzoic acids (DHB), the API displays different hydrogen bonding patterns in different co-crystals. Scheme 4 depicts all the hydrogen bonding synthons observed in the co-crystals of theophylline and dihydroxybenzoic acids.[83]

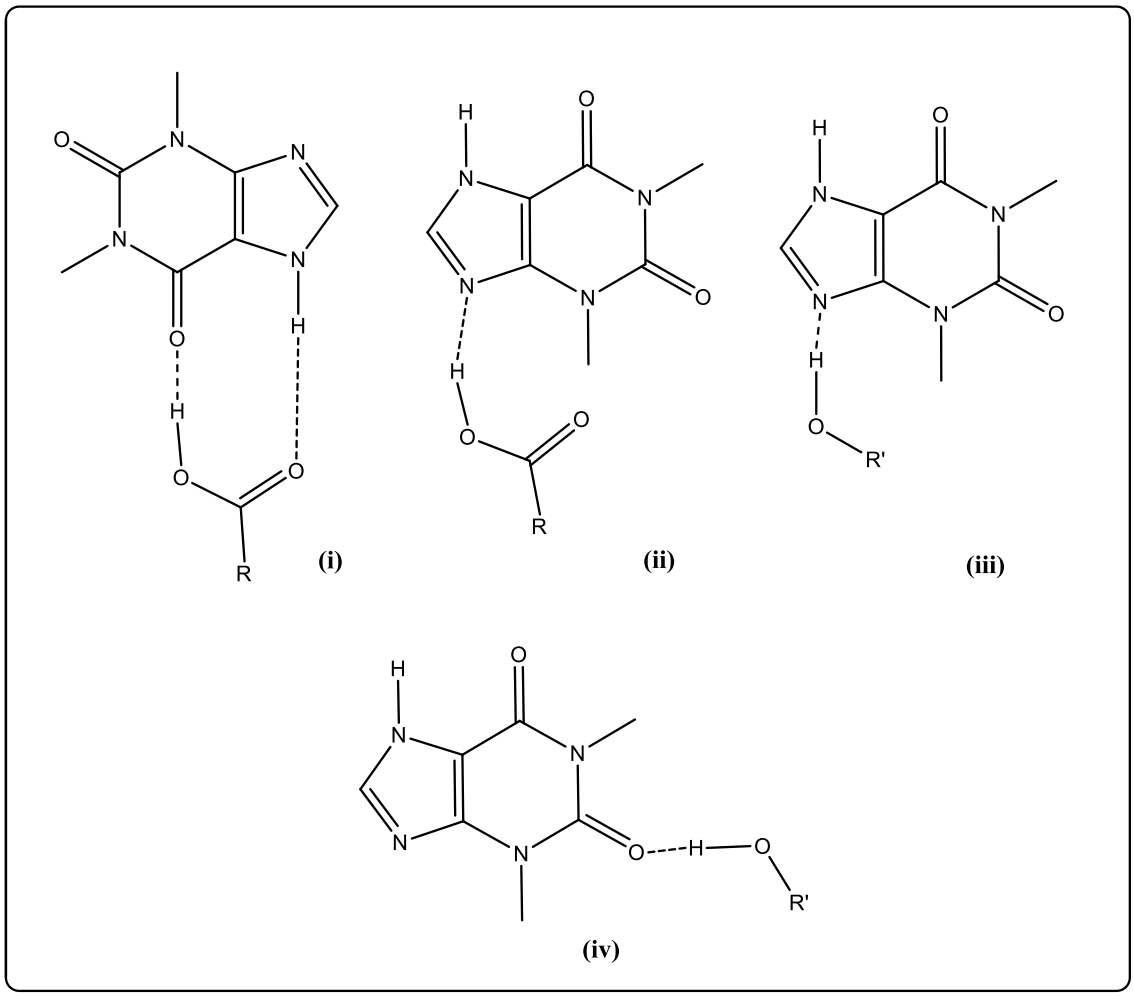

Scheme 4: Selected hydrogen bonding motifs observed in co-crystals of theophylline and several dihydroxybenzoic acids. (i) Ring motif of N-H$_{(imidazole)}$···O=C$_{(carbonyl)}$ and O-H$_{(hydroxyl)}$···O=C$_{(amide)}$. (ii) O-H$_{(carboxylic\ hydroxyl)}$···N$_{(imidazole)}$ (iii) O-H$_{(hydroxyl)}$···N$_{(imidazole)}$ (iv) O-H$_{(hydroxyl)}$···O=C$_{(amide)}$.

According to literature there were two synthons observed repeatedly in multiple structures: the N-H$_{(imidazole)}$···O=C$_{(amide)}$ ring observed in Form **IV** of theophylline (Scheme 3c) and an N-H$_{(imidazole)}$···O=C$_{(carbonyl)}$, O-H$_{(hydroxyl)}$···O=C$_{(amide)}$ cyclic array(Scheme 4i).[83] It is likely there is competition between these synthons during the formation of the co-crystals. When studying only the interactions between the API and co-former in TPL·DHB co-crystals (Table 4) homointeraction 3c is observed in 60% of the structures and interaction (i) is observed in the other 40%. Bučar and co-workers[83] did a study on the synthons in hydroxybenzoic acid co-crystals of theophylline and also reported the same trend.

Table 4: Observed interactions between theophylline and various dihydroxybenzoic acid co-formers.

Co-former	Interactions*	REFCODE
2,3-dihydroxybenzoic acid	i and iii	DOPNAZ[83]
2,4-dihydroxybenzoic acid	i and iii	DOPNAD[83]
2,5-dihydroxybenzoic acid	ii, iv and c	DUCROJ[83]
3,4-dihydroxybenzoic acid	ii, iv and c	WOCHON[78]
3,5-dihydroxybenzoic acid	ii, iv and c	WOCHIH[78]

*Numbers refer to diagrams in Scheme 4 and letters refer to Scheme 3.

The presence of so many different synthons in co-crystals of theophylline with various dihydroxybenzoic acids indicates that theophylline co-crystals may be susceptible to synthon polymorphism. In this work, various known co-crystals of theophylline with different dihydroxybenzoic acids were screened for polymorphism. These co-crystals were chosen because of the synthon diversity noted in the co-crystals of theophylline and the dihydroxybenzoic acids. Theophylline was used because it has multiple hydrogen bond donor and acceptors which could interact with the DHBs in different was thus leading to synthon polymorphs. Also, theophylline is structurally very similar to caffeine which has multiple polymorphic co-crystals and it was hoped theophylline would also be as prone to co-crystals polymorphism. Only the co-crystals of theophylline and 3,4-dihydroxybenzoic acid was found to be polymorphic and is reported in this work. The other failed polymorphism screens are reported in the digital appendix B.

4.2. Polymorphic Co-Crystal of Theophylline and 3,4-Dihydroxybenzoic acid.

In previous studies [78, 83] a co-crystal of theophylline and 3,4-dihydroxybenzoic acid (3,4-DHB) was reported. In the present work the co-crystal (Form **I**) was resynthesized along with a novel polymorph of the co-crystal (Form **II**).

4.2.1. Experimental

Synthesis of diffraction quality crystals of the previously known co-crystal **1** was achieved by slow evaporation from a solution of 1:4 methanol/chloroform (5 ml) and equimolar amounts of theophylline (0.0300 g) and 3,4-DHB (0.0261 g). Bulk samples were prepared by solvent-assisted grinding (with acetonitrile) using stainless steel jar in a Retsch MM200 mixer mill at 25Hz for 10 mins.

Form **II** was initially prepared by slow evaporation at ambient temperatures from a solution of 1:4 methanol/chloroform (5 ml) and equimolar amounts of theophylline (0.0298 g) and 3,4-DHB (0.0245 g). This yielded diffraction quality crystals. However, subsequent attempts to resynthesize **II** using the aforementioned method resulted in **I**. The new form essentially disappeared for a year until it was synthesized again (reproducibly) via two methods. The first method is crystallization from solution (1:4 methanol/chloroform) at 80°C. The second method is crystallization in ethanol in the presence of polyethylene at ambient temperatures. Once **II** has formed it is stable at ambient temperatures.

Both forms were characterised using PXRD, SXRD and thermal techniques. Crystallographic data pertaining to the two polymorphs is summarised in Table 5. Bulk formation of the co-crystals was confirmed using PXRD (Supporting information: Figures S1 and S2)

Table 5: Crystallographic Data for Forms I and II of (TPL)·(3,4-DHB)

Polymorph	**I**	**II**
Chemical formula	$C_{14}H_{14}N_4O_6$	$C_{14}H_{14}N_4O_6$
M_r	334.29	334.29
Crystal system, space group	Triclinic, $P\bar{1}$	Orthorhombic, *Pbca*
Temperature (K)	293	173
a, b, c (Å)	8.0998 (3), 8.6294 (3), 11.6014 (4)	6.7095 (3), 13.7764 (6), 30.7205 (15)
α, β, γ (°)	102.915 (2), 105.069 (2), 105.647 (2)	90.00, 90.00, 90.00
V (Å^3)	715.41 (4)	2839.6 (2)
Z	2	8
Radiation type	Mo $K\alpha$	Mo $K\alpha$
μ (mm^{-1})	0.12	0.13
Crystal size (mm)	0.71 × 0.37 × 0.34	0.39 × 0.12 × 0.07
Data collection		
Diffractometer	Bruker *APEX*-II CCD diffractometer	Bruker *APEX*-II CCD diffractometer
Absorption correction	Multi-scan SADABS [72]	Multi-scan SADABS [72]
No. of measured, independent and observed [$I > 2\sigma(I)$] reflections	8285, 3450, 2862	16504, 3518, 2067
R_{int}	0.043	0.078
$(\sin\theta/\lambda)_{max}$ (Å^{-1})	0.661	0.667
Refinement		
$R[F^2 > 2\sigma(F^2)]$, $wR(F^2)$, S	0.051, 0.163, 1.15	0.049, 0.164, 0.84
No. of reflections	3450	3518
No. of parameters	218	219
No. of restraints	0	0
H-atom treatment	H atoms treated by constrained refinement	H atoms treated by constrained refinement
$\Delta\rho_{max}$, $\Delta\rho_{min}$ (e Å^{-3})	0.88, −0.39	0.22, −0.24

4.2.2. Crystal Structures of the polymorphs of (TPL)·(3,4-DHB)

The asymmetric units of the two polymorphs both contain one molecule of TPL and one molecule of 3,4-DHB as seen in Figure 20.

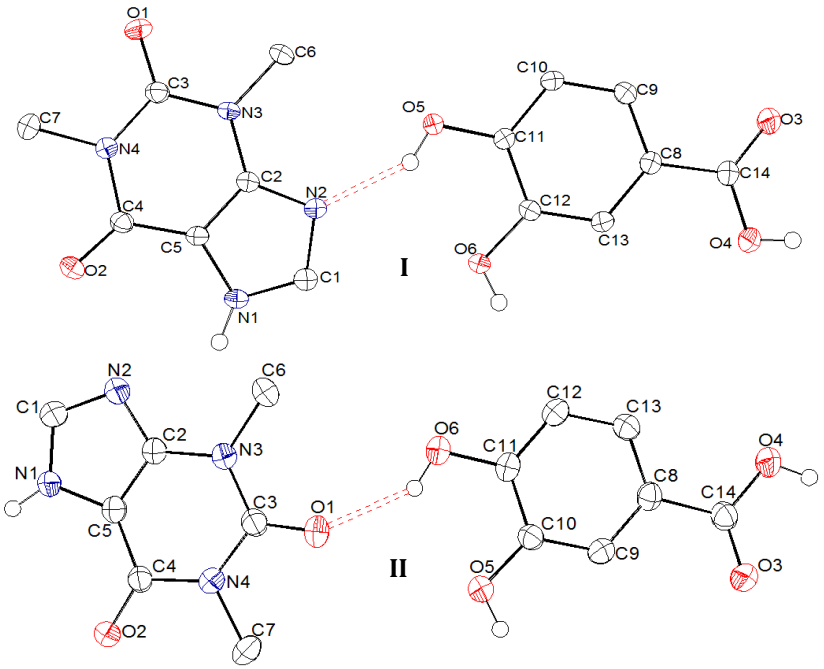

Figure 20: Asymmetric units of Forms I and II of the (TPL)·(3,4-DHB) co-crystal. The atomic numbering in the crystal structures is shown along with the non-symmetry related hydrogen bonding (indicated by the red dashed lines).

As reported by Sarma *et. al.*[78] and Bučar, *et. al.*[83] the crystal structure of **I** contains the robust carboxylic acid dimer along with the TPL dimer formed by the N-$H_{(imidazole)}\cdots O{=}C_{(amide)}$ heterosynthon. Also, in the structure are other interactions between the acid and the API. There is an O-$H\cdots O{=}C_{(urea)}$ heterosynthon and a O-$H\cdots N_{(imidazole)}$ heterosynthon. These interactions are represented by the red dashed bonds in Figure 21. This hydrogen bonding scaffolding leads to the formation of planar sheets within the co-crystal.

Form **II** has different motifs in the crystal. The robust TPL and carboxylic acid dimers are not observed in this form. Instead, there is a cyclic array formed between the carboxylic acid and the TPL via an O-$H_{(carboxylic\ acid)}\cdots O{=}C_{(amide)}$ and N-$H_{(imidazole)}\cdots O{=}C_{(carboxylic\ acid)}$ interactions. This means that the polymorphs of (TPL)·(3,4-DHB) are synthon polymorphs. For this co-crystal, the targeted synthon

polymorph was indeed formed. Form **II** also displays different packing; unlike **I,** it does not crystallise in 2D planar sheet instead the molecules pack in corrugated sheets (Figure 21).

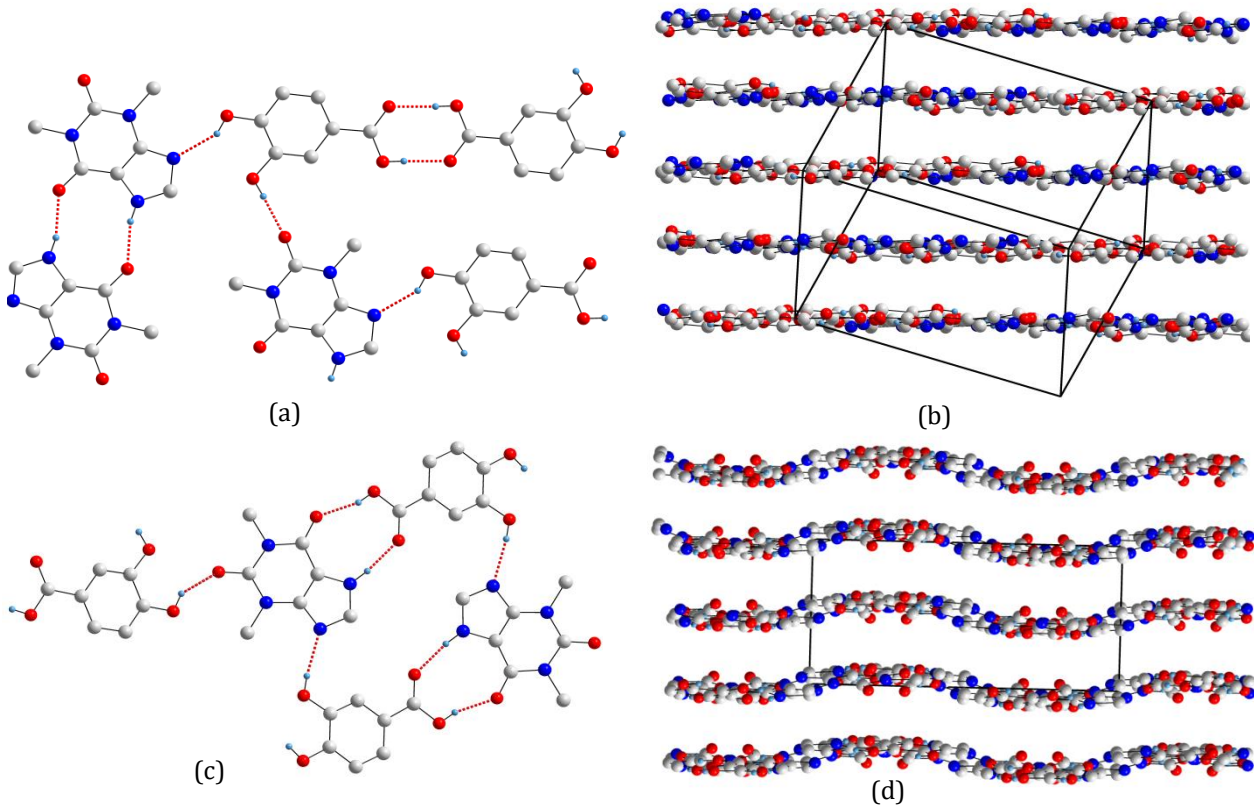

Figure 21: Hydrogen bonding patterns in the polymorphs of the co-crystal (Theophylline)·(3,4-dihydroxybenzoic acid). The red dashed lines represent hydrogen bonds and hydrogen atoms were excluded for clarity.(a) Hydrogen bonding in form I of the co-crystal. (b)Packing in I. (c). Hydrogen bonding in form II of the co-crystal. (d) Packing in II.

4.2.3. Thermal Studies of (TPL)·(3,4-DHB) Polymorphs.

Thermal characterization of polymorphs is one way to categorise polymorphs. Thus far the Roman numerals used to denote the polymorphs have been used without clarification. The previously known form has been called Form **I** because it is more thermally stable than the novel Form **II**. Upon heating at 10°/min, **I** undergoes no phase transitions or changes of any kind until it melts at a temperature of 250.5°C (Table 6). The DSC trace (Figure 22) also shows that soon after this melting point the co-crystal decomposes.

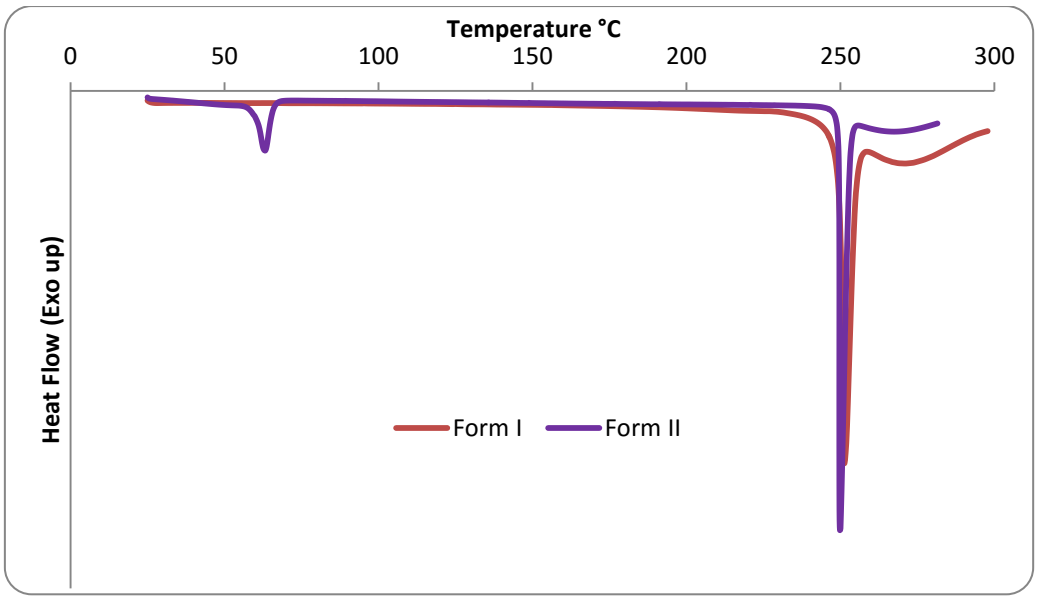

Figure 22: DSC traces of the polymorphs of (TPL)·(3,4-DHB). The red trace shows the heating of Form I and the purple trace shows the response of Form II to heating and a phase transition (from II to I) at 63.2°C is observed.

Table 6: Temperatures of the melting and transition endotherms.

	Melting endotherm		Transition endotherm	
	T_{onset} °C	T_{peak} °C	T_{onset} °C	T_{peak} °C
I	249.5	250.5	N/A	N/A
II	249.5	249.9	59.9	63.2

Upon heating **II** transforms into **I** over a long temperature range. Due to this slow transformation, the DSC trace of Form **II** was obtained at a faster heating rate than the DSC experiment of **I** at 20°/min. With the faster heating rate, the transition temperature of **II** to **I** was observed at 63.2°C. In the DSC experiments once **II** had transformed into **I** there are no more transitions observed until **I** melts at 249.9°C and decomposes soon thereafter. The decomposition is seen in both DSC traces of **I** and **II** as an endothermic hump soon after the sharp melting point.

The phase transition is not reversible. This was observed by heating the **II** crystals high enough to induce the phase transition but not high enough to melt the resulting **I** crystals. Upon cooling **I** crystals that formed and did not convert into **II**, thus,

indicating that the phase transition is not reversible. A cooling run was performed on the melted crystals of **II** (that transformed into **I**) and a phase transition from **I** to **II** was not observed in the trace.

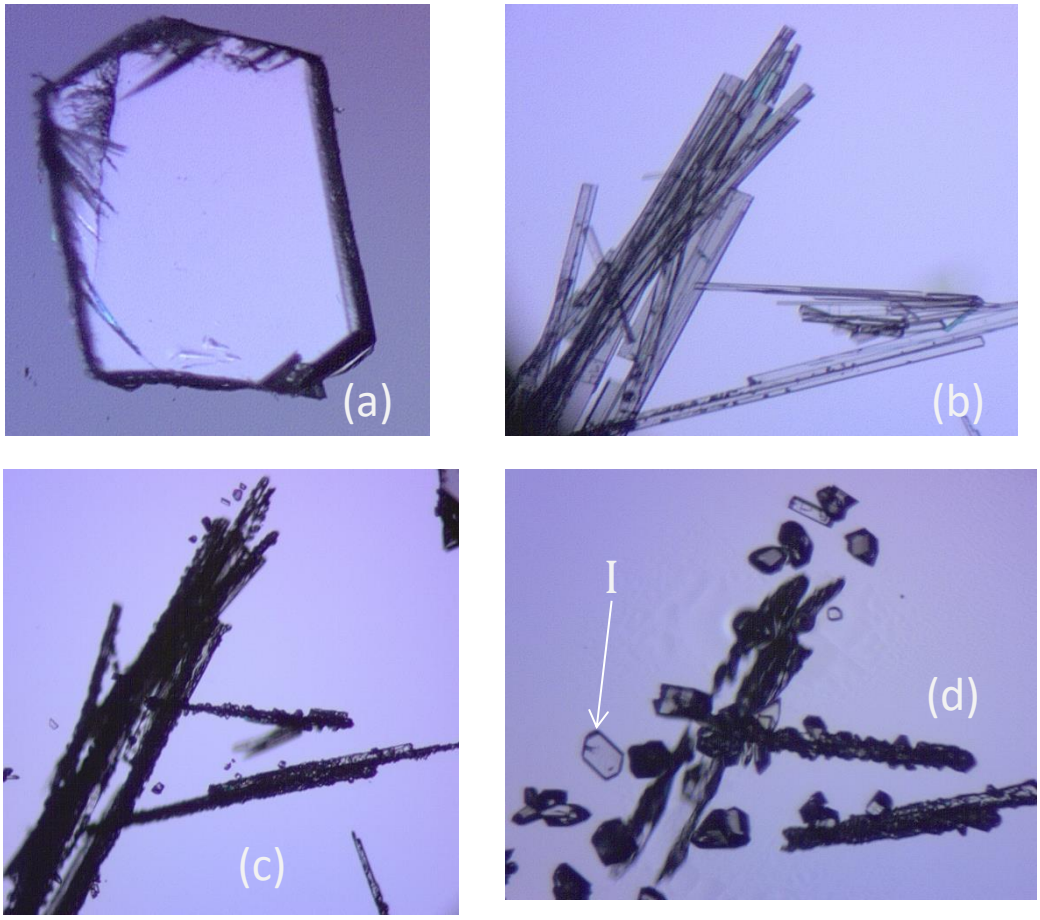

Figure 23:Thermal analysis of the different polymorphs of theophylline·3,4-dihydroxybenzoic acid performed on a hotstage. (a) Block morphology of form I of the co-crystal. (b) Needle morphology of form II of the co-crystal. (c) Heating of Form II lead to needles darkening as phase transition occurs. (d). Form I blocks formed from the form II needles upon further heating.

The transition was also monitored using HSM. The polymorphs of (TPL)·(3,4-DHB) crystallized in two different morphologies. Form **I** crystallized in large blocks (Figure 23a) and **II** produced thin needles (Figure 23b). When the needles of **II** were heated a slow phase transition occurred over a long temperature range (105°C - 216°C). As the transformation began the clear needles of **II** (Figure 23a) darkened (Figure 23c)

and with more heating blocks of **I** visibly grew from the needles of **II** (Figure 23d). The transition is not a single crystal to single crystal transformation.

The Burger-Ramberger rules were applied in order to properly classify the relationship between the polymorphs as either enantiotropic or monotropic. The relationship between these two synthon polymorphs is enantiotropic because the phase transition is endothermic.[38]

5. Co-crystal of Carbamazepine

5.1. Introduction

Pharmaceutically active compound carbamazepine (5*H*-dibenz[*b,f*]azepine-5-carboxamide) has well-documented antiepileptic and analgesic behaviour.[84] Carbamazepine is also known to form at least four different polymorphs as well as an expanding number of hydrates, solvates, and co-crystals.[85] Carbamazepine has a rigid molecular framework which means that structural changes in its multi-component crystals is mostly due to intermolecular changes rather than intramolecular changes. This makes it an ideal candidate for a synthon polymorphism study.

In the various polymorphs of pure carbamazepine, there is a dimer-forming homosynthon (Scheme 5). This dimer is also present in many of the carbamazepine co-crystals salts and other crystalline forms.[85] This dimer is observed in 33% of the 156 carbamazepine co-crystals studied by Childs *et. al.*[85] The co-former in those 156 co-crystals all contained a carboxylic acid moiety. This indicates that the dimer is very robust but also that in some case the dimer can be broken.

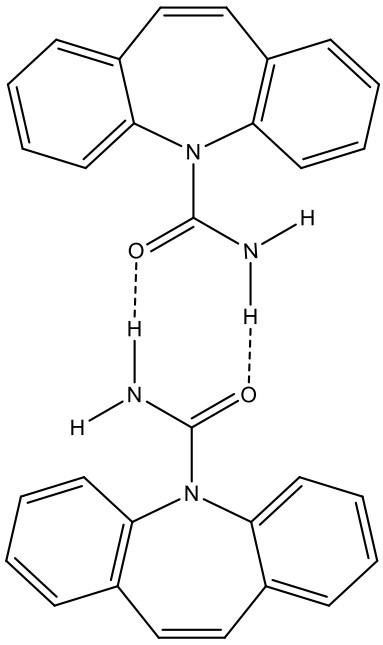

Scheme 5: Carbamazepine dimer forming urea···urea homosynthon.

In the case of polymorphic co-crystal carbamazepine·4-hydroxybenzoic acid,[85] the dimer is present in form **I** of the co-crystal (Figure 24a) and is not formed in the other polymorph. Form **II** possess a $C^2_2(6)$ hydroxyl···carboxamide chain that links the API to the carboxylic acid (Figure 24b).

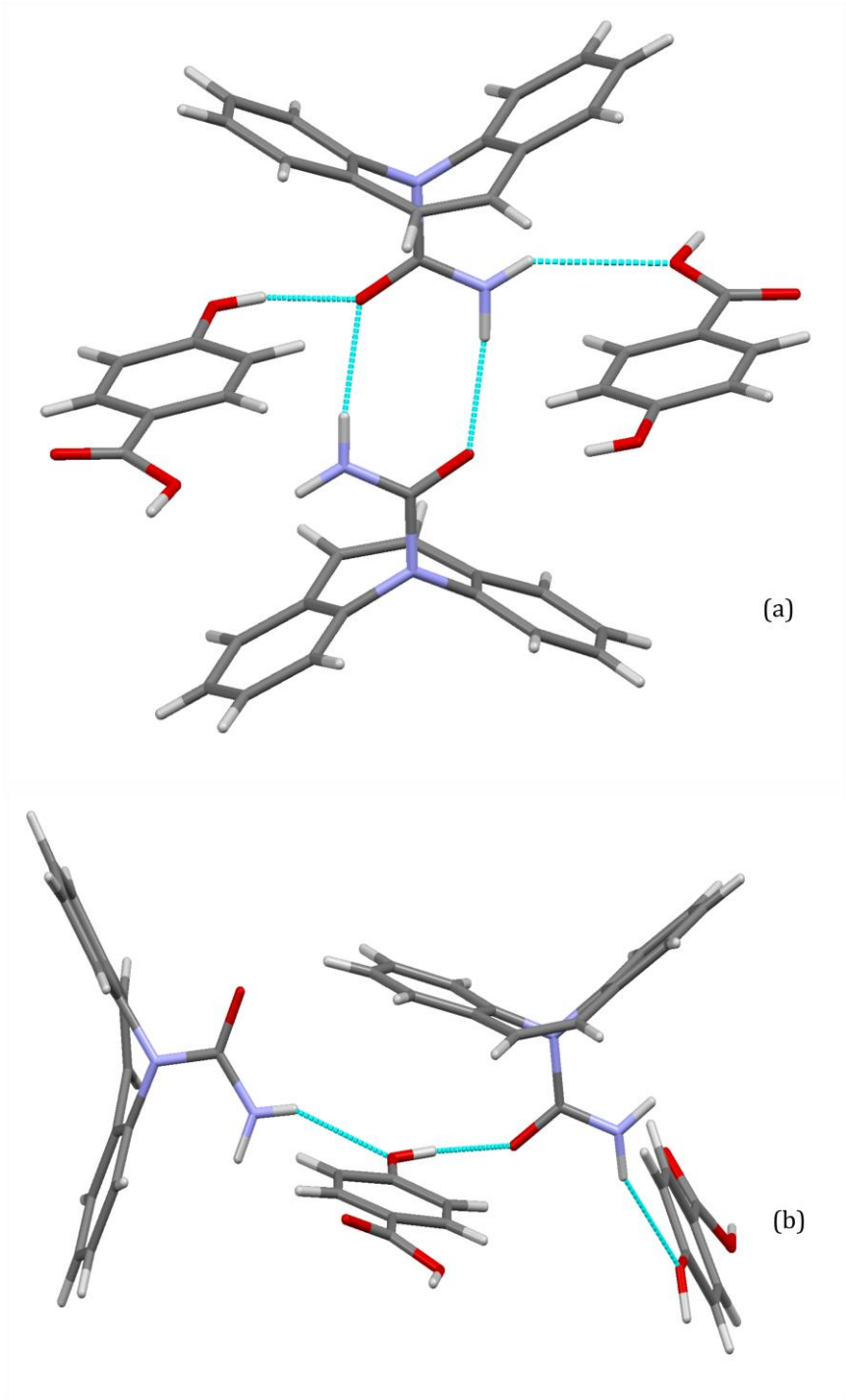

Figure 24: (a) Carbamazepine dimer observed in carbamazepine·4-hydroxybenzoicacid form I co-crystals. (b) Heterosynthon observed in carbamazepine·4-hydroxybenzoicacid form II co-crystals. [85]

In previous experimental studies[25, 86] it was indicated that carbamazepine does form co-crystals with cinnamic acid. This co-crystal was reported as a powder and the possible synthon framework holding the co-crystal together was predicted using 3D modelling by Moradiya and co-workers (Figure 25).[86] It predicted that the co-crystal of carbamazepine and cinnamic acid has an $R^2_2(8)$ interaction between the carboxylic acid of cinnamic acid and the amide of carbamazepine. In this work, we attempted to grow the reported co-crystal in order to know what synthons are present in this co-crystal as well as to possibly grow the polymorph of that co-crystal.

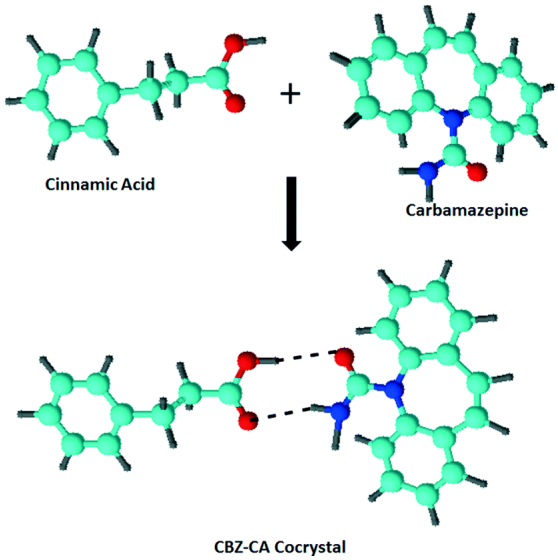

Figure 25: Intermolecular interactions of the carbamazepine·cinnamic acid co-crystal that were predicted by Moridiya et al. (2014). Picture taken from ref [86].

5.2. Co-crystal: Carbamazepine•Cinnamic acid

5.2.1. Experimental

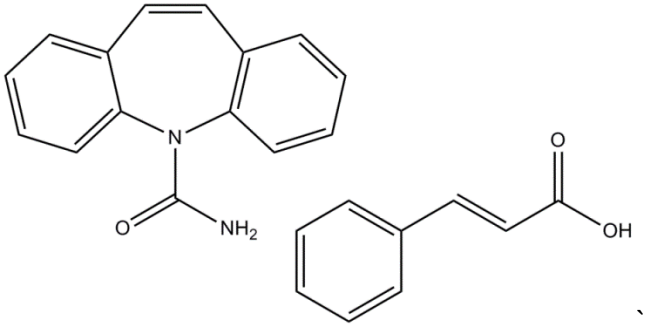

Scheme 6: Carbamazepine and Cinnamic acid.

Anhydrous carbamazepine form **III** was obtained from Sigma-Aldrich and cinnamic acid (form **II**) was obtained from the British Drug House. Both chemicals were characterised by PXRD. The co-crystal was synthesized by forming a 1:1 slurry of carbamazepine (0.0199 g) and cinnamic acid (0.0123 g) in ethyl acetate (0.1 ml). The slurry was sonicated in a sonic bath at 30°C for 17 hrs. Diffraction quality crystals were formed in the bath and were stored in the fridge upon removal from the bath. The data collection and refinement details are tabulated in Table 7. Bulk formation of the crystal was confirmed using PXRD.

Table 7: Crystallographic data for (carbamazepine)·(cinnamic acid)

Crystal data	
Chemical formula	$C_{15}H_{12}N_2O \cdot C_9H_8O_2$
M_r	384.42
Crystal system, space group	Monoclinic, $P2_1/c$
Temperature (K)	173
a, b, c (Å)	15.2149 (5), 5.4351 (2), 23.5139 (10)
β (°)	95.488 (2)
V (Å^3)	1935.56 (13)
Z	4
Radiation type	Mo $K\alpha$
μ (mm^{-1})	0.09
Crystal size (mm)	0.33 × 0.18 × 0.16
Data collection	
Diffractometer	APEX-II CCD
Absorption correction	Multi-scan SADABS[72]
No. of measured, independent and observed [$I > 2\sigma(I)$] reflections	18633, 4670, 3000
R_{int}	0.059
$(\sin \theta/\lambda)_{max}$ (Å^{-1})	0.661
Refinement	
$R[F^2 > 2\sigma(F^2)]$, $wR(F^2)$, S	0.048, 0.152, 1.07
No. of reflections	4670
No. of parameters	263
No. of restraints	0
H-atom treatment	H-atom parameters constrained
$\Delta\rho_{max}$, $\Delta\rho_{min}$ (e Å^{-3})	0.21, −0.28

5.2.2. Powder Analysis

The co-crystal of carbamazepine and cinnamic acid was obtained successfully, and visual inspection of the calculated and measured PXRD data was used to confirm bulk formation of the co-crystal (Figure 26). The calculated pattern was generated using the single crystal data in *Mercury*.[56, 57] The match in patterns confirms that the bulk material is the same as the single crystal that was analysed.

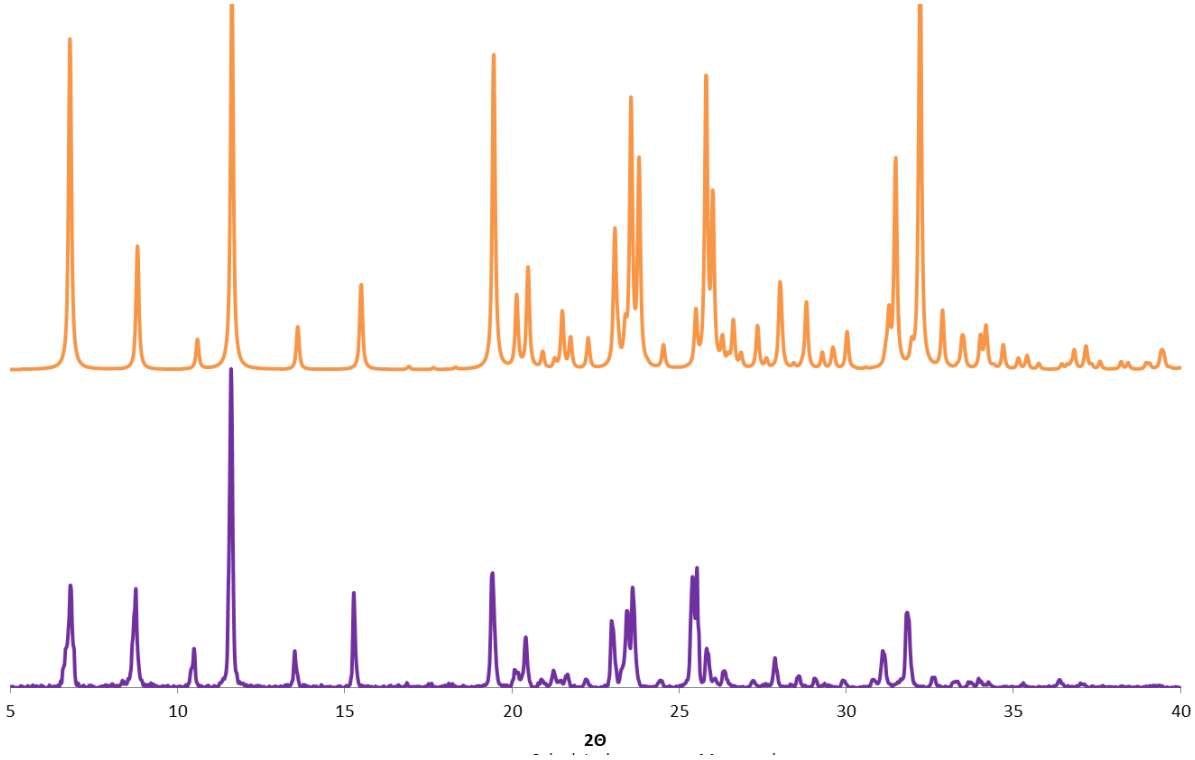

Figure 26: PXRD patterns of the carbamazepine·cinnamic acid co-crystal synthesized in this work: (a) Measured powder pattern of the co-crystal (measured using cobalt radiation). (b) Calculated powder pattern of carbamazepine·cinnamic acid co-crystal using cobalt radiation.

The PXRD patterns generated by Shayanfar *et. al.*[25] and Moradiya *et. al.*[86] were obtained using copper radiation; the pattern that was measured in this work was obtained using cobalt radiation. This being the case the measured pattern could not be directly compared to the patterns in literature. To confirm that the co-crystal formed is the same as the one reported in the literature, the literature patterns were compared to a pattern that was calculated from single crystal data using copper radiation as the source in *Mercury* (Figure 27).[56, 57] This could be done because single crystal was shown to be that same as the bulk material. Visual inspection of the

patterns confirmed that the synthesized co-crystal was the co-crystal reported by Shayanfar *et. al.*[25] and Moradiya *et.al.*[86]

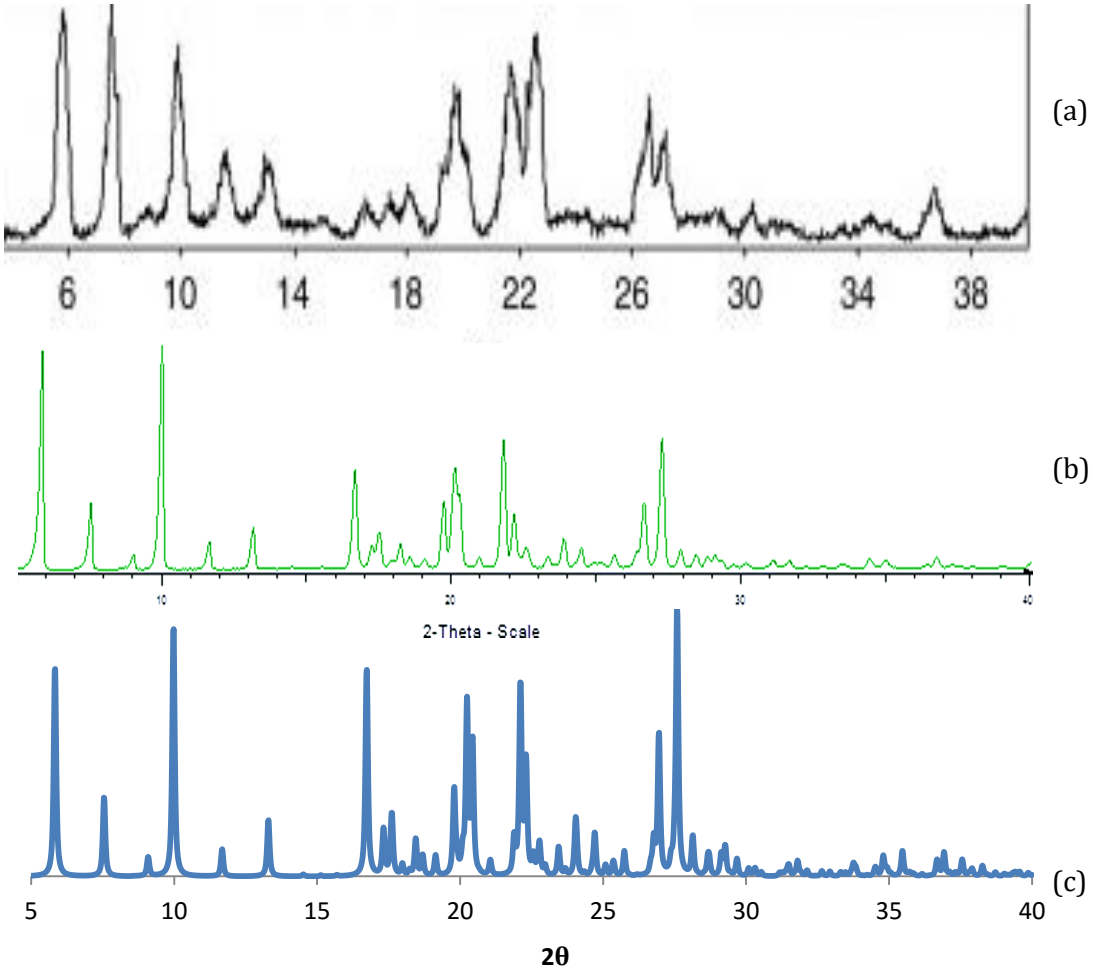

Figure 27: Powder patterns of the carbamazepine·cinnamic acid co-crystal taken from different sources: (a) Carbamazepine·cinnamic acid co-crystal powder pattern taken from ref 25. (b) Carbamazepine·cinnamic acid co-crystal powder pattern taken from ref 88. (c) Calculated powder pattern of carbamazepine·cinnamic acid co-crystal using copper radiation.

5.2.3. Thermal Analysis

Thermal analysis by differential scanning calorimetry further confirmed the formation of the co-crystal. The average melting point, calculated using three DSC thermograms is 143.7°C. This melting point is different from the melting points of carbamazepine (191-192°C) and cinnamic acid (132-135°C). The melting point

reported in the literature are 144°C[25] and 143.1°C[86]. This provides further confirmation that the co-crystal formed is the one reported in the two studies. Figure 28 shows a representative DSC thermogram of the carbamazepine·cinnamic acid co-crystal. This DSC trace is not flat because the crystals sublime as they get heated up. The melting endotherm in this trace was at 142.5°C.

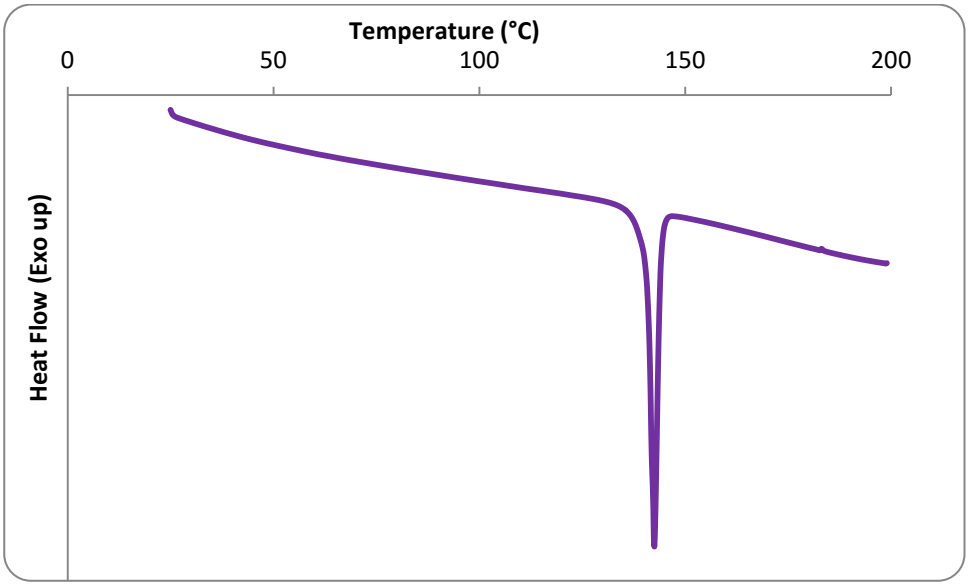

Figure 28: DSC thermogram of co-crystal of cinnamic acid and carbamazepine.

5.2.4. Structural Analysis

The asymmetric unit cell of the co-crystal contains a carbamazepine molecule and one cinnamic acid molecule and is shown in Figure 29.

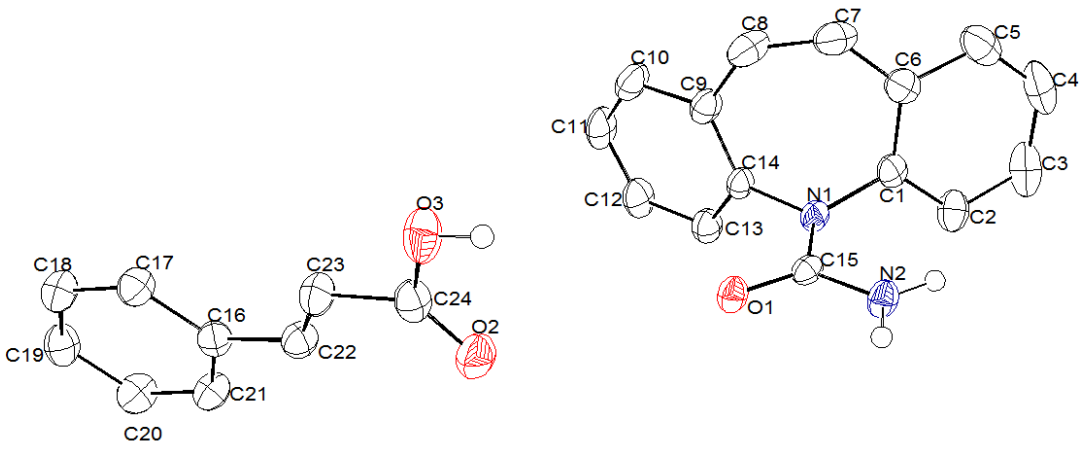

Figure 29: The asymmetric unit of the co-crystal with the displacement ellipsoid drawn at 50% probability level.

In the co-crystal two molecules of carbamazepine form a dimer across an inversion centre via an $R^2_2(8)$ urea homosynthon, as seen in Figure 30. This dimer is observed in many of the co-crystals of carbamazepine and in its four polymorphs.[85] The cinnamic acid molecules interact with carbamazepine to form an $R^4_4(16)$ ring. This is achieved with two sets of O-H$_{(carboxylic\ acid)}$···O=C$_{(urea)}$ and N-H$_{(urea)}$···O=C$_{(carboxylic\ acid)}$ heterosynthon interactions. These intermolecular interactions do not correspond with the ones predicted by Moradiya *et al.* (2014).[86] The co-crystal of carbamazepine and cinnamic acid was shown to be sustained by different synthons than the ones predicted in the literature. The predicted synthon may possibly be obtained using different crystallization techniques and environments.

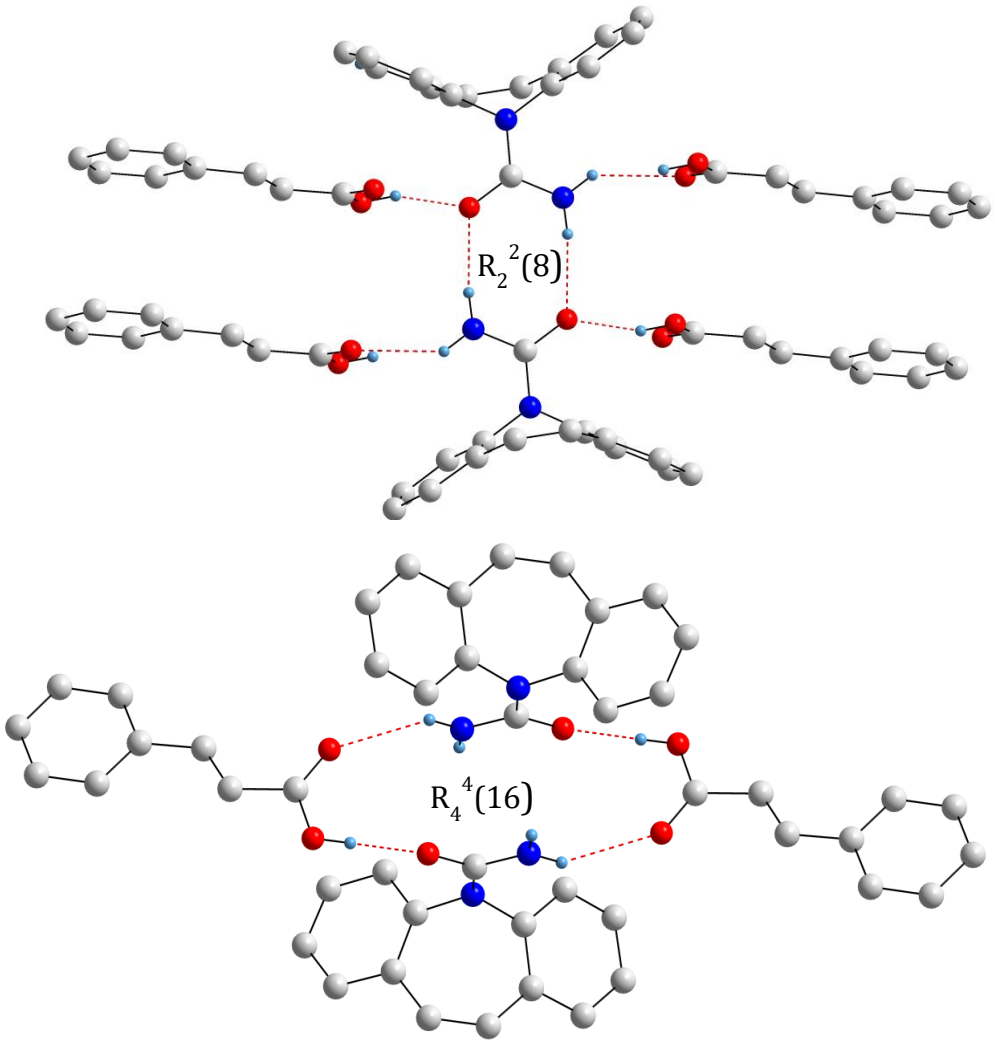

Figure 30**: Hydrogen bonding interactions in carbamazepine·cinnamic acid.**

6. Concluding Remarks

Polymorphism in single component crystals is a phenomenon that has been extensively investigated, and it is now gaining interest in multiple component crystals. Polymorphism in co-crystals has been the subject of a several studies and recently more polymorphic co-crystals have been reported.

6.1. Remarks on the data mining

The quantity of polymorphic co-crystals in the CSD was investigated and 239 polymorphic co-crystals were obtained. This is only 8% of the 2925 co-crystals that were isolated. When compared with the fact that approximately 50% of the single component crystals that are screened for polymorphism are found to be polymorphic, this makes it seem like co-crystallization decreases the polymorphic potential of co-crystals. However, since the number of targeted single component polymorphic screens is much larger than that of purposeful polymorphic screens of multi-component systems, this results in a biased view

The polymorphs isolated from the CSD were classified by the type of polymorphism. Packing polymorphism was found to be the most prevalent type of polymorphism, followed closely by conformational polymorphism. As in single component crystals, the flexibility of the molecules in the co-crystal seems to play a notable role in the polymorphism of the co-crystal. This is suggested by the high number of conformational polymorphs observed. Even in co-crystals containing rigid molecules, like caffeine, the use of a flexible co-former opened up the possibility of conformation polymorphism which is not present in the crystals of the pure rigid molecules. This implies that one could make polymorphic co-crystals by selecting co-formers of high flexibility.

Tautomeric polymorphs were not observed; this could be a result of excluding zwitterions from the search parameters. A significant number of synthon polymorphs were found and analysis of the types of synthons that are prevalent in these co-crystals may aid targeted attempts to form synthon polymorphs.

Future database searches could provide a better overview of the current state of polymorphism in co-crystals. The many search restrictions that this work was subjected to makes it a narrow view of the big picture. The inclusion of salts and ternary co-crystals may provide better information on the nature of polymorphism in multi-component systems. Since salt formation is driven by strong ionic interactions, the effects of weaker interactions on the packing and polymorphism of the salts could give insight to the role of weaker intermolecular interaction in the formation of the crystal structure.

The introduction of more molecules into a crystal structure may help or hinder the crystals ability to form polymorphs. At the present moment there is no data to sway the argument in any particular direction. A database analysis that includes co-crystals with more than two components could shed a little bit of light on the subject, if the co-crystals were studied along with their corresponding counterparts which have lower number of components. This could also give insight into the potential hierarchies of competitive intermolecular interactions.

6.2. Targeted attempts to form synthon polymorphs

The addition of extra intermolecular interactions that inherently comes with co-crystallization increases the chances of observing synthon polymorphism. Even though these may be theoretically possible there is no guarantee that they will occur.

6.2.1. Theophylline co-crystals

The presence of multiple hydrogen bond donors and acceptors in theophylline makes the formation of synthon polymorphs of this API possible. Theophylline shows synthon polymorphism in its single-component and multi-component states. Synthon polymorphism was observed in the 1:1 co-crystal of theophylline and 3,4-dihydroxybenzoic acid. The polymorphs of the co-crystal were found to be enantiotropically related due to the endothermic transition.

Future studies of the relative stability of these co-crystals can be carried out with slurry experiments at different temperatures. This work shows that targeted synthon polymorphism can be achieved. Further investigation of other theophylline co-

crystals with dihydroxybenzoic acids may also prove to contain the same type of synthon polymorphism.

6.2.2. Carbamazepine co-crystals

Carbamazepine has many known co-crystals and it has been shown that the carbamazepine homodimer can be interrupted by carboxylic acid moieties. Future work into screening of synthon polymorphism in carbamazepine·carboxylic acid systems may yet prove successful. This kind of work could provide an understanding of the conditions that lead to co-crystal polymorphism for carbamazepine at the very least.

There is ample room for investigation in the realm of polymorphism in multi-component systems and with there being approximately 3000 neutral organic co-crystals in a database with over 800000 (and counting) crystal structures, it is clear that there is not enough data on these type of molecules. Thus, it would be premature and very difficult to obtain a one size fits all summation of the state of polymorphism in co-crystals.

References

1. N. Qiao, M. Li, W. Schlindwein, N. Malek, A. Davies and G. Trappitt, *International Journal of Pharmaceutics*, 2011, **419**, 1-11.
2. R. Thakuria, A. Delori, W. Jones, M. P. Lipert, L. Roy and N. Rodríguez-Hornedo, *International Journal of Pharmaceutics*, 2013, **453**, 101-125.
3. S. L. Childs, L. J. Chyall, J. T. Dunlap, V. N. Smolenskaya, B. C. Stahly and G. P. Stahly, *Journal of the American Chemical Society*, 2004, **126**, 13335-13342.
4. N. Schultheiss and J.-O. Henck, in *Pharmaceutical Salts and Co-crystals*, The Royal Society of Chemistry, 2012, DOI: 10.1039/9781849733502-00110, pp. 110-127.
5. J. W. Steed, *Trends in Pharmacological Sciences*, 2013, **34**, 185-193.
6. S. Aitipamula, R. Banerjee, A. K. Bansal, K. Biradha, M. L. Cheney, A. R. Choudhury, G. R. Desiraju, A. G. Dikundwar, R. Dubey, N. Duggirala, P. P. Ghogale, S. Ghosh, P. K. Goswami, N. R. Goud, R. R. K. R. Jetti, P. Karpinski, P. Kaushik, D. Kumar, V. Kumar, B. Moulton, A. Mukherjee, G. Mukherjee, A. S. Myerson, V. Puri, A. Ramanan, T. Rajamannar, C. M. Reddy, N. Rodriguez-Hornedo, R. D. Rogers, T. N. G. Row, P. Sanphui, N. Shan, G. Shete, A. Singh, C. C. Sun, J. A. Swift, R. Thaimattam, T. S. Thakur, R. Kumar Thaper, S. P. Thomas, S. Tothadi, V. R. Vangala, N. Variankaval, P. Vishweshwar, D. R. Weyna and M. J. Zaworotko, *Crystal Growth & Design*, 2012, **12**, 2147-2152.
7. N. Biswas, in *Pharmaceutical Salts and Co-crystals*, The Royal Society of Chemistry, 2012, DOI: 10.1039/9781849733502-00128, pp. 128-153.
8. G. R. Desiraju, *Journal of Chemical Sciences*, 2010, **122**, 667-675.
9. A. D. Bond, *CrystEngComm*, 2007, **9**, 833-834.
10. *IUPAC Compendium Of Chemical Terminology* Royal Society Of Chemistry, Cambrige, 2nd edn., 1997.
11. G. L. Amidon, H. Lennernäs, V. P. Shah and J. R. Crison, *Pharmaceutical Research*, 1995, **12**, 413-420.
12. H. G. Brittain, *Journal of Pharmaceutical Sciences*, 2013, **102**, 311-317.
13. A. D. Bond, in *Pharmaceutical Salts and Co-crystals*, The Royal Society of Chemistry, 2012, DOI: 10.1039/9781849733502-00009, pp. 9-28.
14. W. Jones, S. Motherwell and A. V. Trask, *MRS. Bulletin* 2006, **31**, 875-879.
15. G. P. Stahly, *Crystal Growth & Design*, 2007, **1**, 1007-1026.
16. A. M. Chen, M. E. Ellison, A. Peresypkin, R. M. Wenslow, N. Variankaval, D. J. Mathre, P. G. Dormer, D. H. Euler, R. G. Ball, A. Ye, Y. Wang and I. Santos, *Chemical Communications*, 2007, 419-421.
17. N. Variankaval, R. M. Wenslow, J. Murry, R. Hartman, R. Helmy, E. Kwong, S. Clas, C. Dalton and I. Santos, *Crystal Growth & Design*, 2006, **6**, 690-700.
18. D. Good, C. Miranda and N. Rodríguez-Hornedo, *CrystEngComm*, 2011, **13**, 1181-1189.
19. C. B. Aakeröy, S. Forbes and J. Desper, *Journal of the American Chemical Society*, 2009, **131**, 17048-17049.
20. N. Schultheiss and A. Newman, *Crystal Growth & Design*, 2009, **9**, 2950-2967.
21. A. V. Trask, S. Motherwell and W. Jones, *Crystal Growth & Design*, 2005, **5**, 1013-1021.
22. T. Gao, H. Zu and J. Zhang, *Journal of Pharmacy and Pharmacology*, 2011, **13**, 6327-6328.
23. H. G. Brittain, *Crystal Growth & Design*, 2012, **12**, 5823-5832.
24. P. Sanphui, N. R. Goud, U. B. R. Khandavilli and A. Nangia, *Crystal Growth & Design*, 2011, **11**, 4135-4145.
25. A. Shayanfar, K. Asadpour-Zeynali and A. Jouyban, *Journal of Molecular Liquids*, 2013, **187**, 171-176.

26. A. Nangia and G. R. Desiraju, *Acta Crystallographica Section A*, 1998, **54**, 934-944.
27. P. Vishweshwar, J. A. McMahon, J. A. Bis and M. J. Zaworotko, *Journal of Pharmaceutical Sciences*, 2006, **95**, 499-516.
28. G. R. Desiraju, *Crystal Engineering: A Textbook*, World Scientific Publishing Co. Pte. Ltd, 2011.
29. P. Metrangolo and G. Resnati, *Chemistry – A European Journal*, 2001, **7**, 2511-2519.
30. S. Tothadi and G. R. Desiraju, *Chemical Communications*, 2013, **49**, 7791-7793.
31. E. Arunan, G. R. Desiraju, R. A. Klein, J. Sadlej, S. Scheiner, I. Alkorta, D. C. Clary, R. H. Crabtree, J. J. Dannenberg, P. Hobza, H. G. Kjaergaard, A. C. Legon, B. Mennucci and D. J. Nesbitt, *Pure and Appiled Chemistry* 2011, **83**, 1637-1642.
32. G. R. Desiraju, *Angewandte Chemie International Edition*, 2011, **50**, 52.
33. G. A. Jefferey and W. Saenger, *Hydrogen Bonding in Biological Structures*, Springer, Berlin, 1991.
34. A. Nangia, *Accounts of Chemical Research*, 2008, **41**, 595-604.
35. G. R. Desiraju, *Angewandte Chemie*, 1995, **34**.
36. A. J. Cruz-Cabeza and J. Bernstein, *Chemical Reviews*, 2013, **114**, 2170-2191.
37. J. D. Dunitz and J. Bernstein, *Accounts of Chemical Research*, 1995, **28**, 193-200.
38. B. Rodríguez-Spong, C. P. Price, A. Jayasankar, A. J. Matzger and N. Rodríguez-Hornedo, *Advanced Drug Delivery Reviews*, 2004, **56**, 241-274.
39. J. D. Dunitz, *Acta Crystallographica Section B*, 1995, **51**, 619.
40. S. Aitipamula, P. S. Chow and R. B. H. Tan, *CrystEngComm*, 2014, **16**, 3451-3465.
41. P. Purohit and P. Venugopalan, *Resonance*, 2009, **14**, 882-893.
42. A. Grunenberg, J.-O. Henck and H. W. Siesler, *International Journal of Pharmaceutics*, 1996, **129**, 147-158.
43. J. Bernstein, *Polymorphism in Molecular Crystals*, Oxford University Press, Oxford, 2002.
44. A. M. Thayer, *Journal*, 2007, **85**, 17.
45. N. J. Babu, L. S. Reddy, S. Aitipamula and A. Nangia, *Chemistry – An Asian Journal*, 2008, **3**, 1122-1133.
46. S. Wishkerman and J. Bernstein, *Chemistry – A European Journal*, 2008, **14**, 197-203.
47. A. Lemmerer, D. A. Adsmond, C. Esterhuysen and J. Bernstein, *Crystal Growth & Design*, 2013, **13**, 3935-3952.
48. S. L. Morissette, Ö. Almarsson, M. L. Peterson, J. F. Remenar, M. J. Read, A. V. Lemmo, S. Ellis, M. J. Cima and C. R. Gardner, *Advanced Drug Delivery Reviews*, 2004, **56**, 275-300.
49. R. J. Davey, N. Blagden, G. D. Potts and R. Docherty, *Journal of the American Chemical Society*, 1997, **119**, 1767-1772.
50. B. R. Sreekanth, P. Vishweshwar and K. Vyas, *Chemical Communications*, 2007, DOI: 10.1039/b700082k, 2375-2377.
51. S. L. Childs and K. I. Hardcastle, *Crystal Growth & Design*, 2007, **7**, 1291-1304.
52. S. Skovsgaard and A. D. Bond, *CrystEngComm*, 2009, **11**, 444-453.
53. F. Allen, *Acta Crystallographica Section B*, 2002, **58**, 380-388.
54. S. Aitipamula, P. S. Chow and R. B. H. Tan, *Crystal Growth & Design*, 2010, **10**, 2229-2238.
55. H. D. Clarke, K. K. Arora, H. Bass, P. Kavuru, T. T. Ong, T. Pujari, L. Wojtas and M. J. Zaworotko, *Crystal Growth & Design*, 2010, **10**, 2152-2167.
56. I. J. Bruno, J. C. Cole, P. R. Edgington, M. Kessler, C. F. Macrae, P. McCabe, J. Pearson and R. Taylor, *Acta Crystallographica Section B*, 2002, **58**, 389-397.
57. C. F. Macrae, I. J. Bruno, J. A. Chisholm, P. R. Edgington, P. McCabe, E. Pidcock, L. Rodriguez-Monge, R. Taylor, J. van de Streek and P. A. Wood, *Journal of Applied Crystallography*, 2008, **41**, 466-470.
58. P. K. Goswami, R. Thaimattam and A. Ramanan, *Crystal Growth & Design*, 2013, **13**.
59. M. K. Stanton, S. Tufekcic, C. Morgan and A. Bak, *Crystal Growth & Design*, 2009, **9**.
60. A. Mukherjee and G. R. Desiraju, *Chemical Communications*, 2011, **47**.

61. S. Ghosh, A. Mondal, M. S. R. N. Kira, U. Ramamurty and C. M. Reddy, *Crystal Growth & Design*, 2013, **13**.
62. A. V. Trask, W. D. S. Motherwell and W. Jones, *Chemical Communications*, 2004, DOI: 10.1039/b400978a, 890-891.
63. J. P. Smit and J. Hagen, *J. Chem. Cryst.*, 2015, **45**.
64. T. Leyssens, N. Tumanova, K. Robeyns, N. Candoni and S. Veesler, *CrystEngComm*, 2014.
65. N. Schultheiss, S. Bethune and J.-O. Henck, *CrystEngComm*, 2010, **12**, 2436-2442.
66. A. L. Grzesiak and A. J. Matzger, *Inorganic Chemistry*, 2007, **46**, 453-457.
67. M. Lang, A. L. Grzesiak and A. J. Matzger, *Journal of the American Chemical Society*, 2002, **124**, 14834-14835.
68. W. W. Porter Iii, S. C. Elie and A. J. Matzger, *Crystal Growth & Design*, 2008, **8**, 14-16.
69. C. P. Price, A. L. Grzesiak and A. J. Matzger, *Journal of the American Chemical Society*, 2005, **127**, 5512-5517.
70. Bruker, *Journal*, 2007.
71. Bruker, *Journal*, 2001.
72. G. M. Sheldrick, *Journal*, 1997.
73. G. Sheldrick, *Acta Crystallographica Section A*, 2008, **64**, 112-122.
74. G. M. Sheldrick, *SHELXL-2014, University of Göttingen and Bruker AXS, Karlsruhe* 2014.
75. L. Farrugia, *Journal of Applied Crystallography*, 2012, **45**, 849-854.
76. A. Spek, *Acta Crystallographica Section D*, 2009, **65**, 148-155.
77. W. Pennington, *Journal of Applied Crystallography*, 1999, **32**, 1028-1029.
78. B. Sarma and B. Saikia, *CrystEngComm*, 2014, **16**, 4753-4765.
79. D. Khamar, R. G. Pritchard, I. J. Bradshaw, G. A. Hutcheon and L. Seton, *Acta Crystallographica Section C*, 2011, **67**, o496-o499.
80. K. Fucke, G. J. McIntyre, C. Wilkinson, M. Henry, J. A. K. Howard and J. W. Steed, *Crystal Growth & Design*, 2012, **12**, 1395-1401.
81. Y. Ebisuzaki, P. D. Boyle and J. A. Smith, *Acta Crystallographica Section C*, 1997, **53**, 777-779.
82. S. Zhang and A. Fischer, *Acta Crystallographica Section E*, 2011, **67**, o3357.
83. D.-K. Bučar, R. F. Henry, G. G. Z. Zhang and L. R. MacGillivray, *Crystal Growth & Design*, 2014, **14**, 5318-5328.
84. M. Habgood, M. A. Deij, J. Mazurek, S. L. Price and J. H. ter Horst, *Crystal Growth & Design*, 2009, **10**, 903-912.
85. S. L. Childs, P. A. Wood, N. Rodríguez-Hornedo, L. S. Reddy and K. I. Hardcastle, *Crystal Growth & Design*, 2009, **9**, 1869-1888.
86. H. G. Moradiya, M. T. Islam, S. Halsey, M. Maniruzzaman, B. Z. Chowdhry, M. J. Snowden and D. Douroumis, *CrystEngComm*, 2014, **16**, 3573-3583.

Supporting Information

1.1. Supporting information for TPL 3,4DHB polymorphs

1.2.1. Powder diffraction patterns of Form I and II of TPL·3,4-DHB

The calculated pattern of form I (figure S31) is shifted slightly to the left since, the single crystal data and powder data were collected at different temperatures.

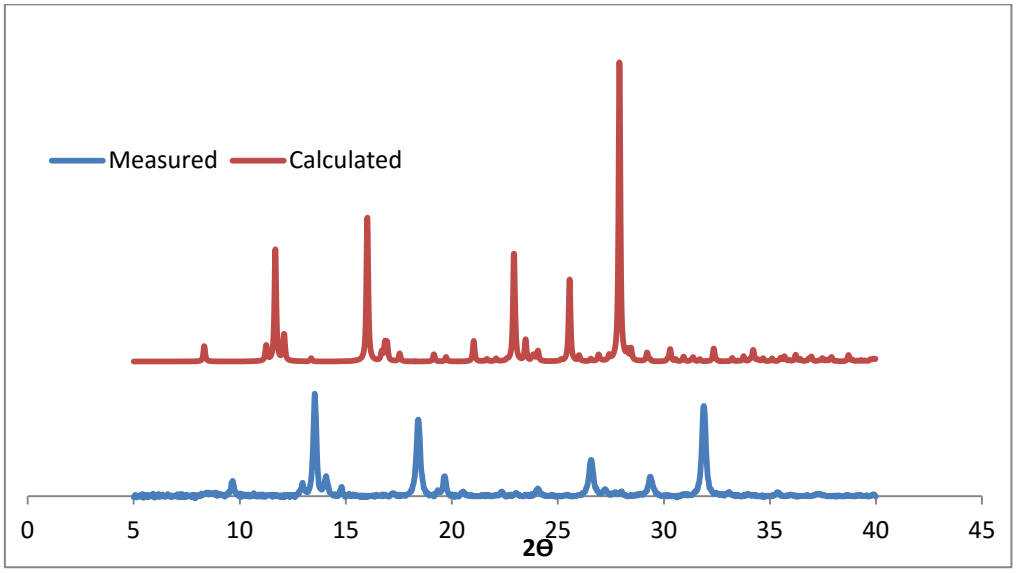

Figure S31: PXRD of TPL·3,4-DHB form I compared to PXRD of single crystal structure determination of TPL·3,4-DHB form. The experimental pattern was calculated at room temperature and the calculated pattern at 173 K.

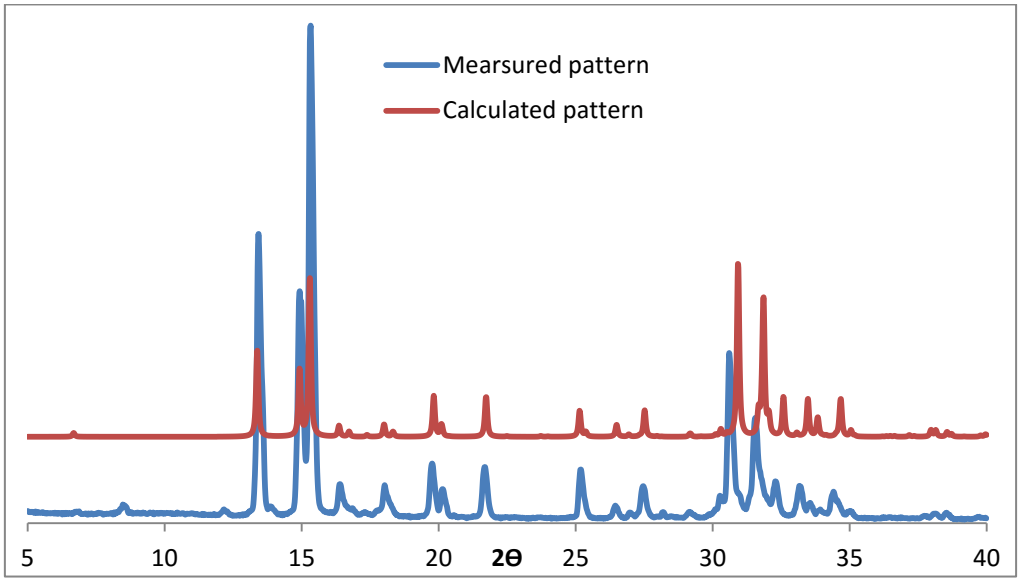

Figure S32: PXRD of TPL·3,4-DHB form II compared to PXRD of single crystal structure determination of TPL·3,4-DHB form. The experimental pattern was calculated at room temperature and the calculated pattern at 173 K